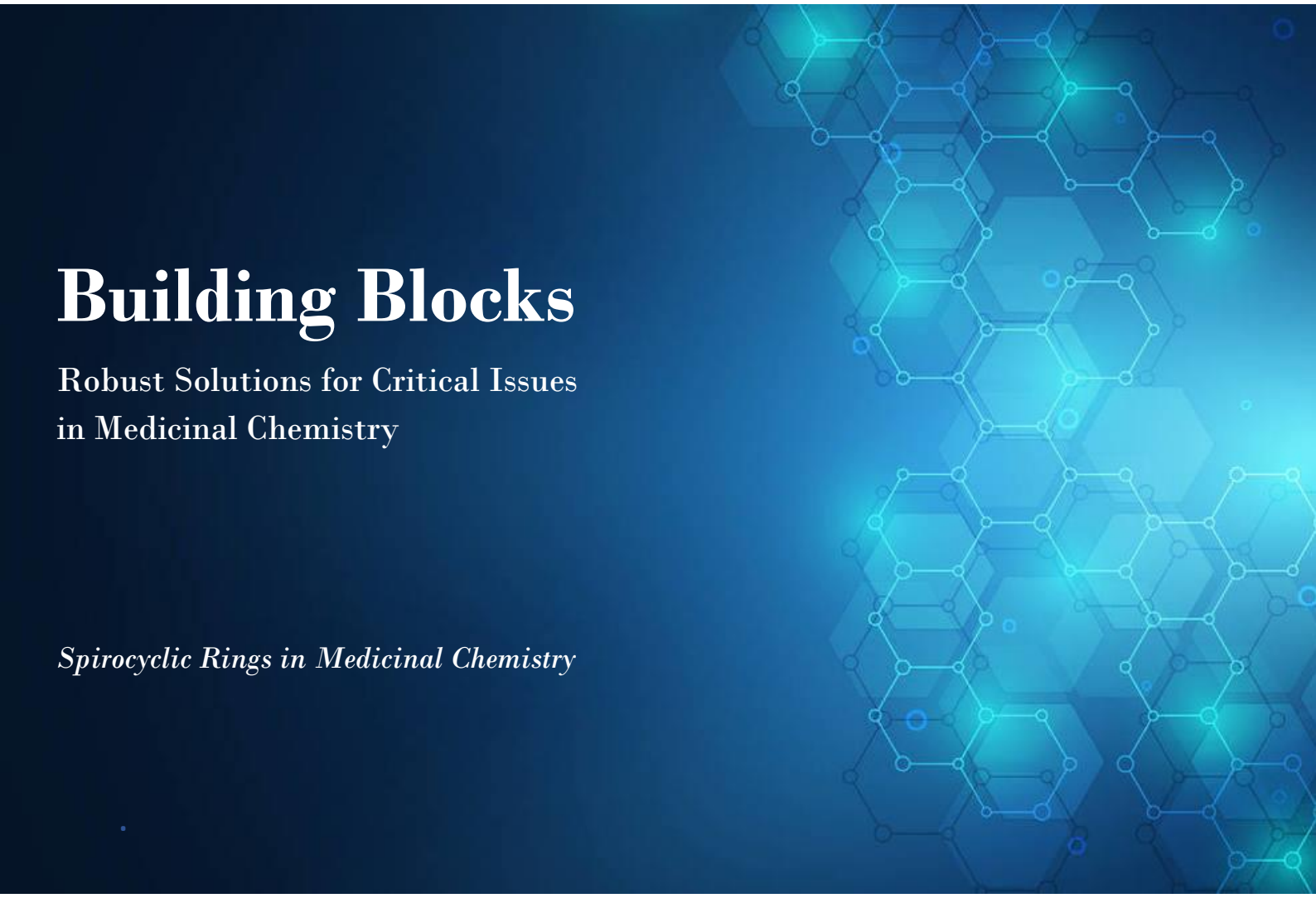

Building Blocks

Robust Solutions for Critical Issues in Medicinal Chemistry

Spirocyclic Rings in Medicinal Chemistry

Spirocyclic Rings in Medicinal Chemistry

Spirocyclic scaffolds are the focus of modern drug discovery, as can be observed by the number of publications and contributions to a variety of approved drugs and clinical candidates (**Figure 79**). Studies that endorse the use of scaffolds with high Fsp^3 further enhance the interest in novel and established spirocycles. The increase in rigidity resulting from spirocyclization can influence important factors, such as potency and selectivity. Furthermore, significant improvements in physicochemical properties, such as logD, lipophilicity and solubility, as well as ADMET properties, are achievable, ultimately leading to improved pharmacokinetic profiles. However, their full potential has not yet been exploited. Methodologies for the systematic exploration of the spirocyclic chemical space are still in their infancy. Taken together, spirocycle is a powerful tool for medicinal chemists with further potential to advance in the near future. As expected, it is often associated with increased synthetic effort, resulting from an increased number of synthetic steps and stereocenters or unusual reaction procedures. Recent advances in the development of synthetic methods and efficient supplies of diverse **spirocyclic building blocks** have allowed the introduction and increase in spirocycles in medicinal chemistry in the past decade. [1-5]

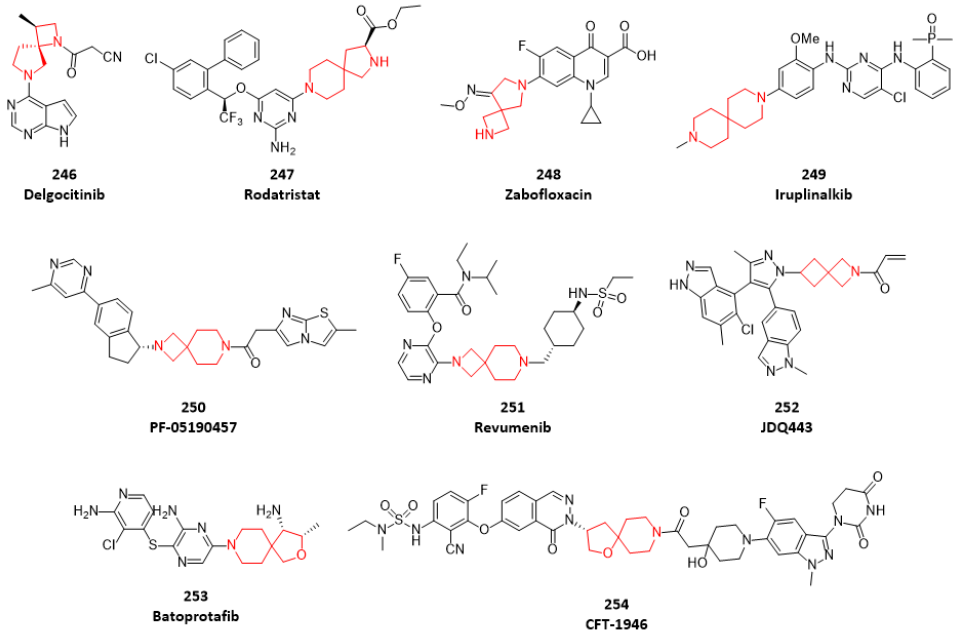

Figure 79. Spirocycles contribute to a variety of approved drugs and clinical candidates.

In order to develop a new series of JAK inhibitors, the team replaced piperidine in approved drug **Tofacitinib** (**255**) with a variety of spirocyclic diamine rings as depicted in **Figure 80**. Replacing pyrrolidine ring in the spirocycle of compound **256** with azetidine ring in the spirocycle of compound **257** increased both cellular potency and metabolic stability in both human and monkey microsomes. Adding a methyl group on azetidine ring in the spirocycle of compound **258** further increased JAK3 inhibition by 4-5 fold compared to compound **257**. It was explained that the methyl group occupied the lipophilic pocket neighborhood the JAK3 hinge region. However, cellular potency was not increased proportionally, and metabolic stability was decreased. Adding two fluorine atoms on azetidine ring in the spirocycle of compound **259** kept comparable potency, but metabolic stability was decreased slightly. Replacing piperidine rings in the spirocycle of compound **259** and **258** with pyrrolidine rings generated compound **260** and **246** (**Delgocitinib**) respectively.

Compound **246** (**Delgocitinib**) has both excellent potency and metabolic stabilities, and was moved into clinical trials. [6]

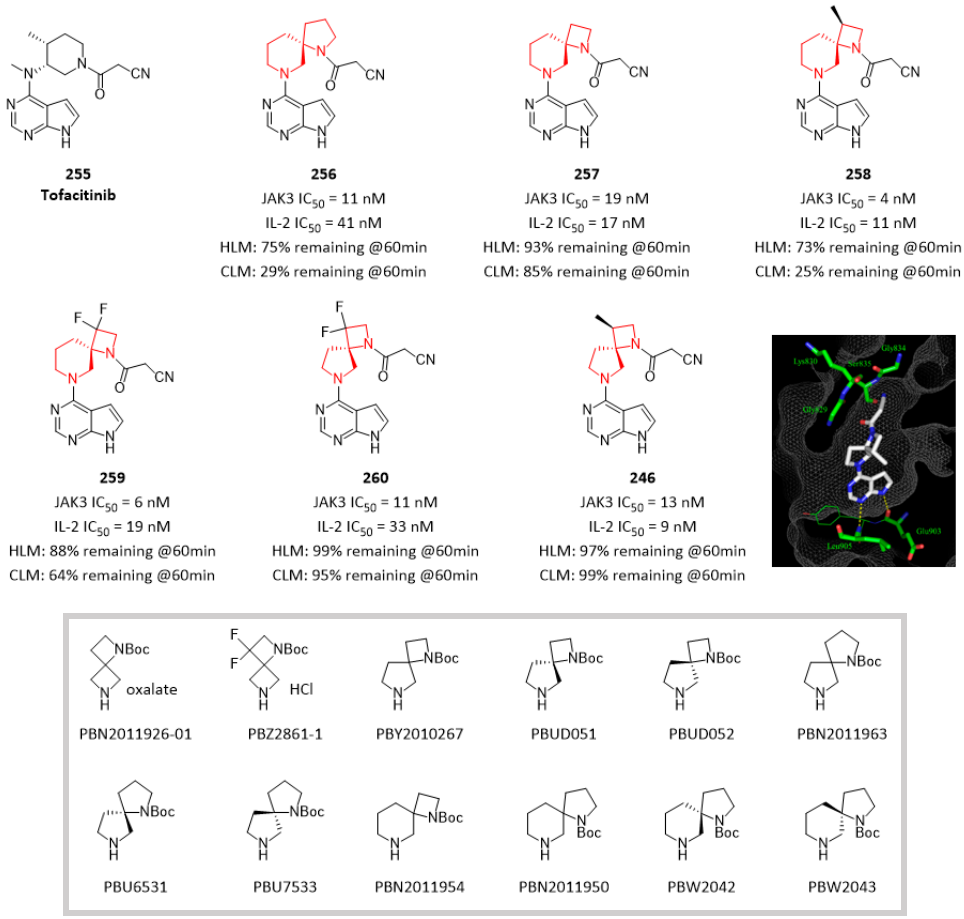

Figure 80. Discovery of JAK inhibitors bearing spirocyclic rings. (PDB code: 7C3N)

In the course of discovery of a novel covalent KRAS G12C inhibitor **JDQ443**, compound **261** was identified as one promising hit compound. Initial SAR exploration aimed to balance specific reactivity toward KRAS G12C versus intrinsic chemical cysteine reactivity. Several drugs containing an acrylamide electrophile have been approved by FDA and demonstrate favorable safety profiles. However, excessively reactive electrophiles increase the risk of nonspecific covalent protein adduct formation and the potential for immune-mediated adverse reactions. Intrinsic chemical reactivity was determined by assessing the disappearance of the compound in the presence of 5 mM reduced GSH, representing a concentration close to intracellular conditions. Compound **261** exhibited modest inhibition of ERK phosphorylation with IC_{50} = 500 nM, but suffered low stability in GSH addition assay with $T_{1/2}$ = 20 min. In compound **262**, replacement of the eletron-withdrawing fluorine atom with a methyl group decreased inhibition of ERK phosphorylation, but stability in GSH addition assay was increased remarkably with $T_{1/2}$ = 107 min. To further optimize the linker geometry and, most importantly, to reduce the intrinsic chemical reactivity of the acrylamide, the team evaluated aliphatic linkers as phenyl replacement. A spiro-azetidine moiety, as in compound **263**, turned out to be the best suitable linker identified. For compound **263**, intrinsic chemical reactivity was significantly lowered with $T_{1/2}$ = 241 min, while reasonable inhibition of ERK phosphorylation was maintained with IC_{50} = 3900 nM. Therefore, the spirocyclic moiety was kept constant in subsequent SAR studies. Further exploration based on compound **263** led to identification of clinical candidate **JDQ443** (**Figure 81**). [7]

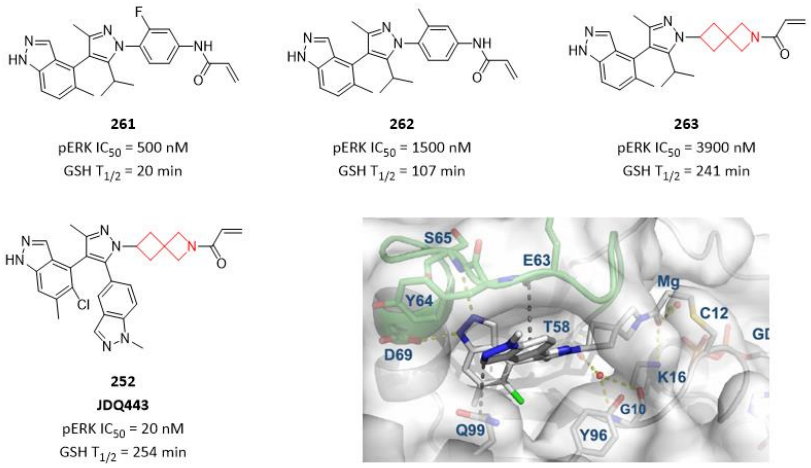

Figure 81. Spriocyclic rings were used in discovery of JDQ443. (PDB code: 7R0M)

In the course of discovery of LSD1 inhibitors, the team examined the impact of linker between the two amines on the activity and ADME properties. A variety of spirocyclic rings were surveyed as linkers in compound **265** (4,6-spiro) and compound **266** (4,4-spiro). Compared to compound **264** (piperidine), two types of spirocyclic rings in compound **265** (4,6-spiro) and compound **266** (4,4-spiro) both increased microsome stabilities in various species, while keeping comparable potency (**Figure 82**). [8]

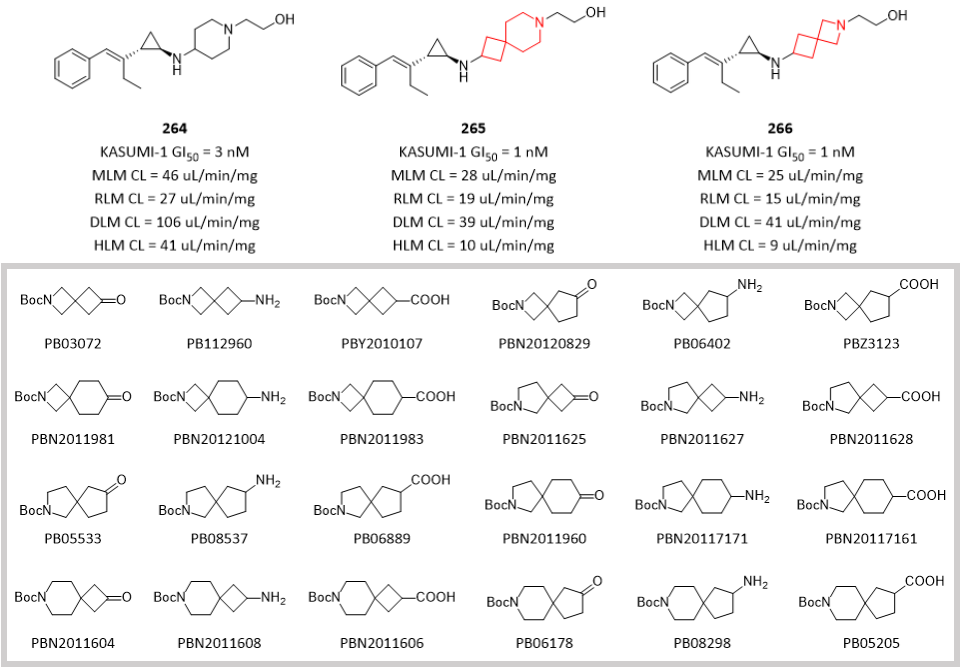

Figure 82. Spriocyclic rings increased microsome stabilities in various species.

Drug repurposing is an economical and effective approach to discover new drugs. Starting from a HTS of an epigenetic inhibitor library, clinical candidate **Quisinostat** (**267**) was revealed as a potent antimalarial agent. However, the extensive inhibitory activity of **Quisinostat** on HDACs results in serious safety issues, which limits its further development as an antimalarial drug. Hence, **Quisinostat** (**267**) was treated as the lead compound for medicinal chemistry investigation to find new chemical entities with good antimalarial efficacy and adequate safety. A conformational restriction and homologues strategy was adopted by replacing the 4-aminomethylpiperidine moiety with a 2,6-diazaspiro[3.4]octane moiety to give compound **268**. As expected, the antimalarial

activity of compound **268** was preserved, and a cell viability assay confirmed that the cytotoxicity of compound **268** indeed decreased considerably with 159-fold and 336-fold safety index (SI) compared with that of **Quisinostat** (**267**). Further optimization by introducing a cyano group on indole ring generated compound **269** with higher antimalarial activity and higher safety index (SI) (**Figure 83**). [9]

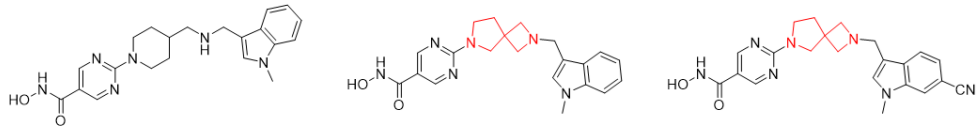

267 (Quisinostat)
3D7 IC_{50} = 4 nM
Dd2 IC_{50} = 7 nM
HepG2 IC_{50} = 30 nM (SI = 8)
293T IC_{50} = 60 nM (SI = 15)

268
3D7 IC_{50} = 4 nM
Dd2 IC_{50} = 4 nM
HepG2 IC_{50} = 720 nM (SI = 159)
293T IC_{50} = 1520 nM (SI = 336)

269
3D7 IC_{50} = 1 nM
Dd2 IC_{50} = 1 nM
HepG2 IC_{50} = 1020 nM (SI = 810)
293T IC_{50} = 1210 nM (SI = 960)

Figure 83. Spirocyclic ring increased safety index.

In order to reduce DNA damage and cytotoxicity of **Olaparib** (**270**), the team examined the pharmacological consequences of replacing the piperazine core in **Olaparib** (**270**) with a variety of diazaspiro systems, in hopes of developing a noncytotoxicity congener of the FDA-approved drug. This work afforded best-in-class compound **271** with a 4,4-spirocyclic ring, an **Olaparib** congener with nanomolar PARP-1 affinity and poor DNA damaging properties, which can be explored as a potential therapeutic for inflammation or neurodegeneration applications where cytotoxicity is not desired. Compound **271** inhibits PARP activity in a manner similar to **Olaparib**. However, compared to the FDA approved drug, higher concentration level of compound **271** was required to completely block PAR synthesis. Compound **271** was unable to induce DNA damage at concentrations as high as 10 uM. These data provide strong evidence that compound **271** showed high PARP-1 affinity and good catalytic inhibitory properties without DNA damaging properties. Compound **272** with a 6,6-spirocyclic ring also reduced DNA damaging and cytotoxicity, but PARP-1 affinity was also decreased by 7-fold compared with **Olaparib** (**270**) (**Figure 84**). [10]

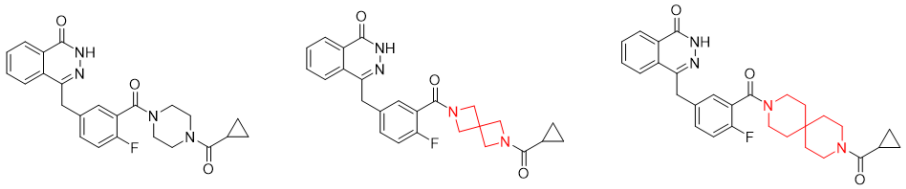

270 (Olaparib)
PARP-1 IC_{50} = 6 nM
Cytotoxicity: 40% @10 uM

271
PARP-1 IC_{50} = 12 nM
Cytotoxicity: 80% @10 uM

272
PARP-1 IC_{50} = 44 nM
Cytotoxicity: 60% @10 uM

Figure 84. Spirocyclic rings reduced DNA damage and cytotoxicity of Olaparib.

In order to discover highly selective dopamine D3 receptor (D3R) antagonists, the team examined a series of diazaspiro alkane cores as depicted in compound **274**-**279**. Compound **273** was a potent D3R antagonist, but selectivity against D2R was modest with SI = 40. Replacing piperazine in compound **273** with various spirocyclic rings in compound **274**-**279** impacted potency and selectivity in a remarkable way. Among of them, 5,5-spirocyclic ring in compound **276**, 6,5-spirocyclic ring in compound **278**, and 6,6-spirocyclic ring in compound **279** kept comparable potency while increasing selectivity significantly. Especially, compound **279** exhibited a high potency with D3R Ki = 12 nM and a high selectivity against D2R with SI = 905 (**Figure 85**). [11]

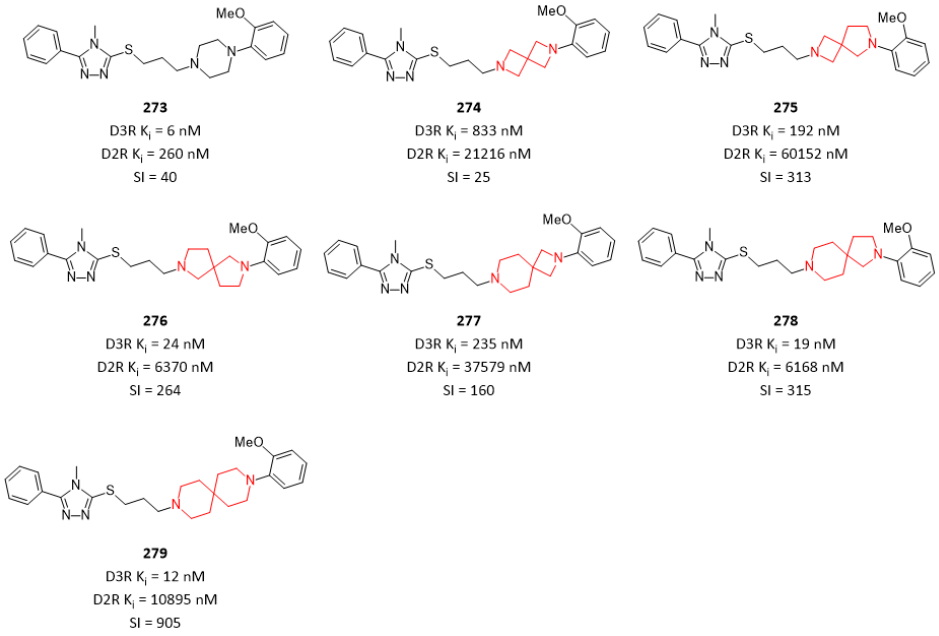

Figure 85. Spirocyclic rings impacted potency and selectivity remarkably.

Two 6,5-spirocyclic rings in compound **281** and **282** respectively, were used as replacements of piperazine ring in compound **280**. Both of them resulted in improvement in the LSD1 inhibitory activity compared with compound **280**. However, compound **281** demonstrated 62% hERG inhibition at 10 uM. It was extremely interesting that compound **282** where nitrogen atom was in a different place had little hERG inhibition with only 10% inhibition at 10 uM (**Figure 86**). [12]

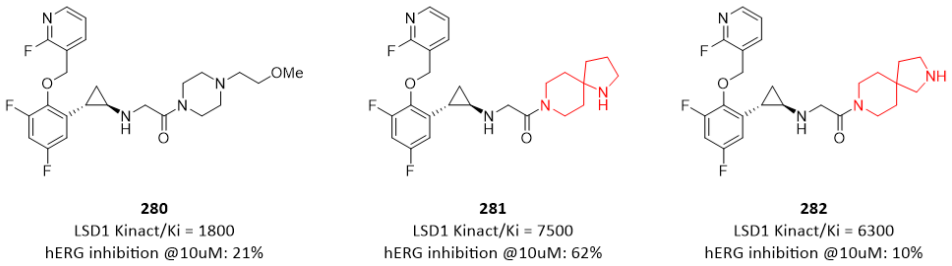

Figure 86. Spirocyclic rings increased potency and decreased hERG inhibition.

As described in above case stories, there is a great variant for diazaspirocylic rings with different ring size, or different orientation resulted from different place of nitrogen atoms. So a diverse library of diazaspirocyclic building blocks is of great value for medicinal chemists to quickly evaluate SAR or SPR in their medicinal programs (**Figure 86**).

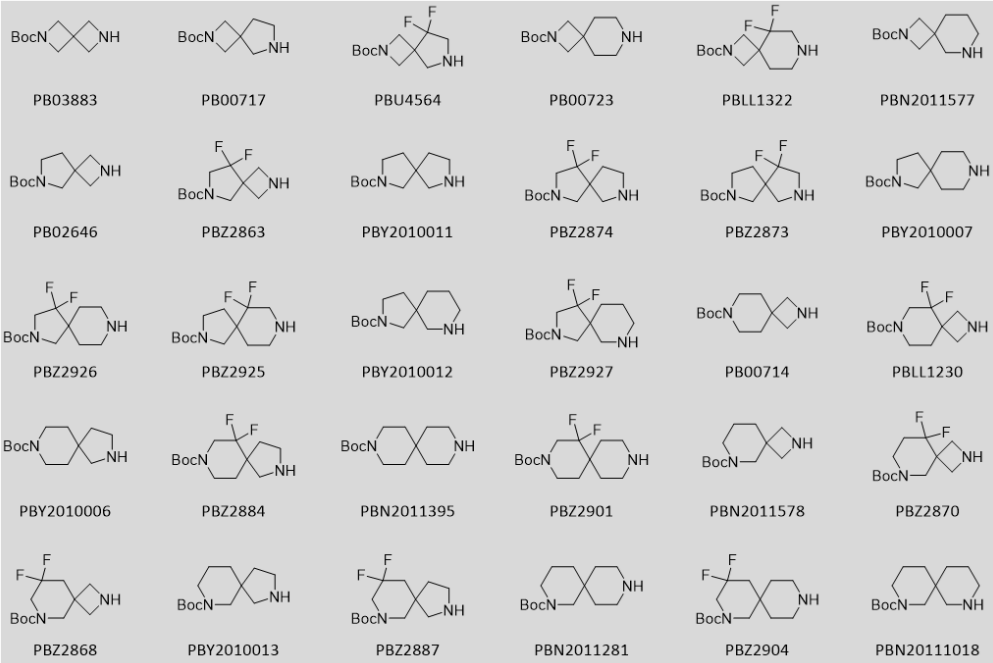

Figure 86. A diverse library of diazaspirocyclic building blocks

Rigidization of the primary amine by a spriocycle has been performed by researcher at Novartis during optimization of SHP2 inhibitors for cancer treatment. Two teams reported on two lead series **283** and **285** respectively, making use of the same spirocyclic rigidization. Both lead series started with compounds bearing a 4-methylpiperidin-4-ylmethanamine moiety, which exhibited very good in vitro potency. However, cellular potency and antiproliferative effects were significantly diminished. X-ray structure analysis revealed that the primary amine group is engaged in three directed hydrogen bond interactions. Rigidization of the aminomethyl moiety could be achieved by introduction of spirocyclic systems carrying the exocyclic amine. All spirocyclic variants, especially compound **284** and compound **286**, exhibited comparable in vitro potency. However, the cellular efficacy was improved by increased lipophilicity (**Figure 87**). [13-14]

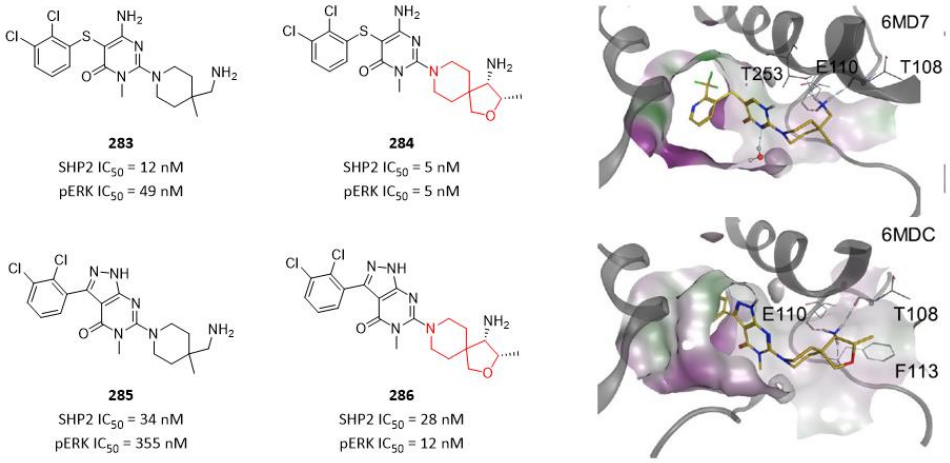

Figure 87. Spirocyclic rings increased potency. (PDB code: 6MD7, 6MDC)

Like diazaspirocyclic rings, oxa-azaspirocyclic rings also have a great variety defined by different ring size, or different orientation resulted from different place of nitrogen and oxygen atoms. So a diverse library of oxa-azaspirocyclic building blocks is of great value for medicinal chemists to

quickly evaluate SAR or SPR in their medicinal programs (**Figure 88**). More interesting case stories where oxa-azaspirocyclic rings have remarkable impacts were discussed below.

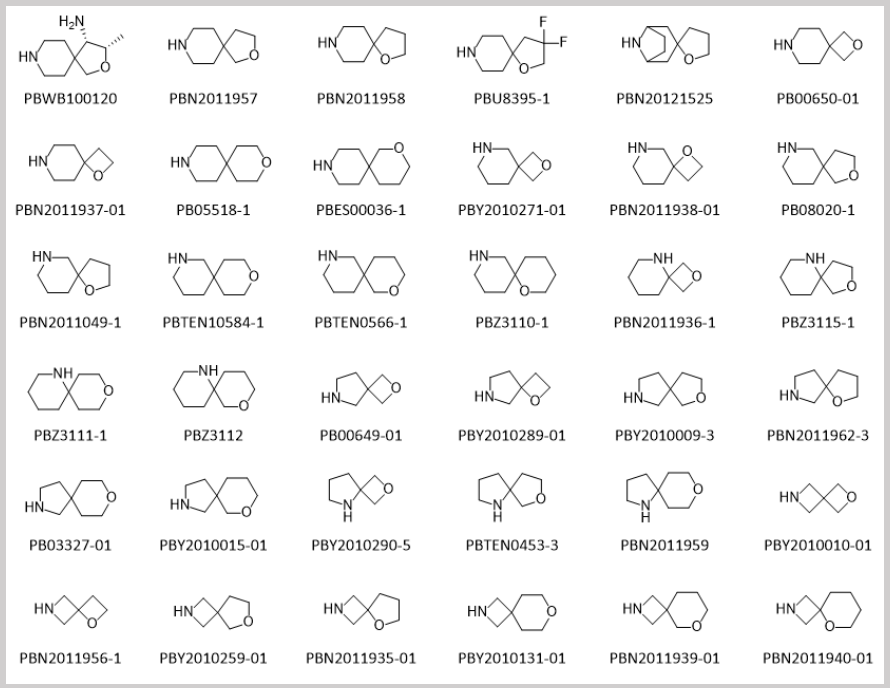

Figure 88. A diverse library of oxa-azaspirocyclic building blocks

In the course of discovery of MCHr1 antagonist **AZD1979** (**290**), the homomorpholine derivative **287** was identified which offered an improvement in properties over morpholines, but metabolic turnover rate was still too high with a high clearance in human microsome. The team's attention was turned to replace homomorpholine ring in compound **281** with some oxa-azaspirocyclic rings in compound **288**, compound **289** and **AZD1979** (**290**). It was interesting to find that compound **288** and compound **290** have decreased clearance in human microsome, while keeping comparable potency (**Figure 89**). [15]

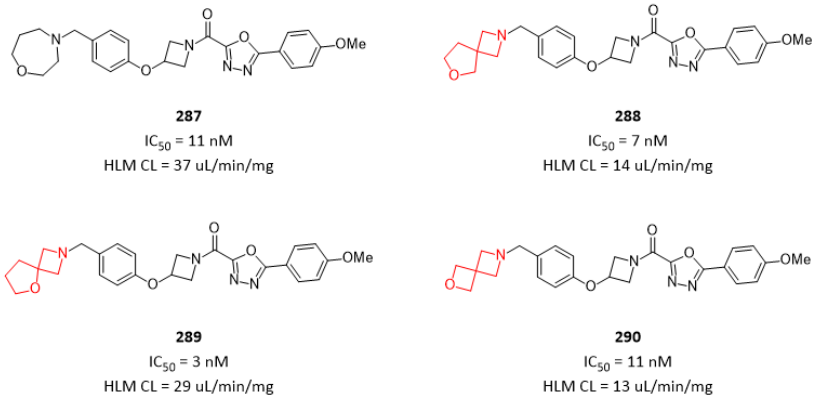

Figure 89. Spirocyclic rings decreased clearance in human microsome.

As the early lead compound, **291** looked very promising. However, particular attention was paid to hERG inhibition which was determined to be 7 uM. The basic lipophilic amine was the most likely contributor to the hERG inhibition. Therefore, strategy focused on reducing basicity of piperidine to decrease hERG inhibition while retaining excellent potency. In compound **292**, a common strategy to introduce fluorine atoms was employed. Indeed, as expected hERG inhibition was decreased remarkably. However, the potency was decreased by 4-fold. In compound **293**, pyrrolidine ring was

used instead of piperidine ring which decreased hERG inhibition while keeping potency. Installation of a sprio-oxetane ring on pyrrolidine in compound **294** decreased hERG inhibition while keeping comparable potency (**Figure 90**). [16]

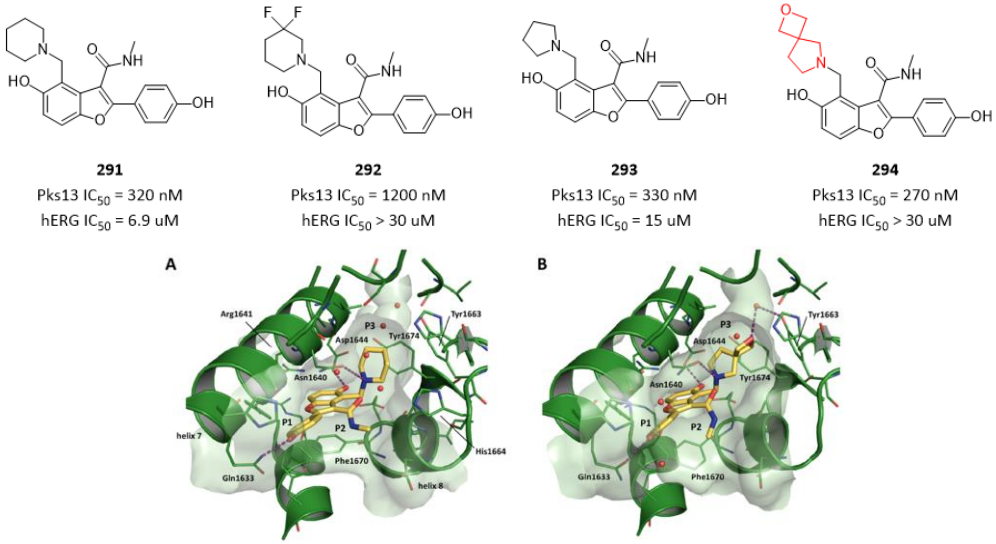

Figure 90. Spirocyclic rings decreased hERG inhibition. (PDB code: 5V3Y and 7M7V)

Compound **295** was identified as a highly potent hDGAT1 inhibitor, but suffered off-target CYP3A4 inhibition with IC_{50} = 6 uM, CYP2C9 inhibition with IC_{50} = 10 uM, and hERG inhibition with IC_{50} = 5 uM. Besides, there was a low solubility issue (< 4 uM) at pH=2 for compound **295**. In order to solve

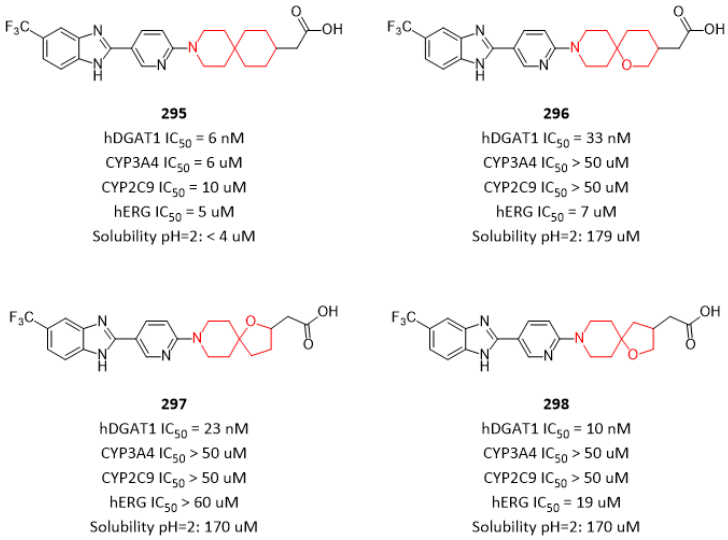

Figure 91. Oxa-spirocyclic rings solved CYP inhibition, hERG inhibition and solubility issues.

these problems, additional oxygen atom was introduced into the spirocyclic ring in compound **296**. Although potency was decreased by 5-fold, compound **296** decreased both CYP3A4 and CYP2C9 inhibition, and increased solubility dramatically. However, hERG inhibition issue was not solved for compound **296**. It was interesting that when ring size was reduced to five-membered tetrahydrofuran in compound **297**, both CYP inhibition and hERG inhibition were not detected, while solubility was increased significantly. Compound **298** also contained a tetrahydrofuran ring, like compound **297**, which decreased both CYP inhibition and hERG inhibition and increased solubility while keeping comparable potency (**Figure 91**). [17]

In many cases, spirocyclic rings brought several issues, such as solubility and metabolic stability, caused by increased number of carbon atoms which made molecule more lipophilic. So, a general strategy is to replace on carbon atom with a polar oxygen atom to balance properties of the whole molecule (**Figure 92**).

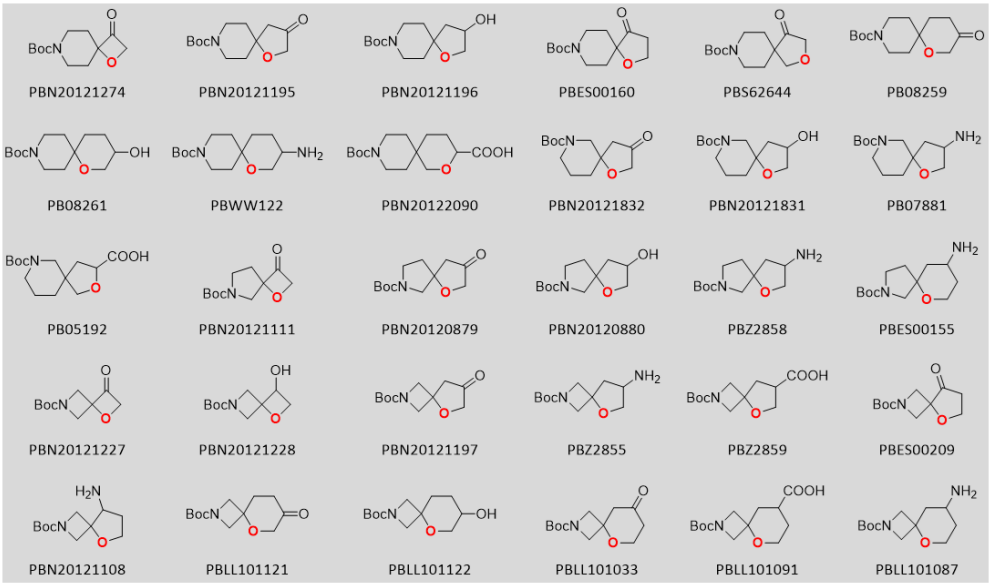

Figure 92. Spirocyclic rings containing a polar oxygen atom in the ring

In order to discover a potent, orally bioavailable small-molecule inhibitor of WNT signaling, the team identified a promising lead compound **299**. With compound **299** in hand, the team decided to further explore the piperidine carboxamide in order to understand the optimal geometry. Although a germinal methyl group in compound **300** decreased potency slightly by 2-fold, it suggested that spirocyclic carboxamides might be tolerated. With this in mind, the spirocyclic ring in compound **301** kept potency, while additional carbonyl in compound **302** resulted in a very potent inhibitor caused by improved hydrogen bond donor ability (**Figure 93**). [18]

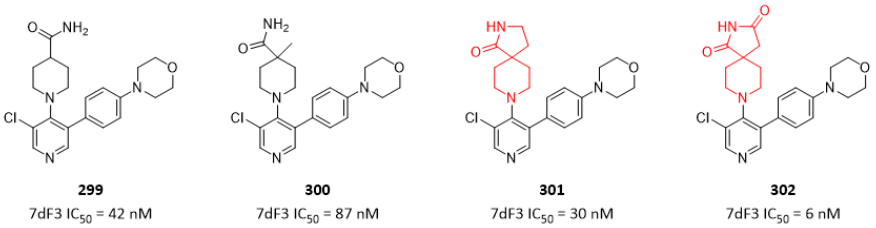

Figure 93. Spirocyclic amide increased potency

Spriocyclic amides were used in discovery of selective dual TYK2/JAK1 inhibitor **303**, where NH of lactam formed a key hydrogen bond with protein. In compound **304**, a selective CYP11B2 inhibitor, oxygen of carbonyl of lactam formed a key hydrogen bond with protein (**Figure 94**). [19-20]

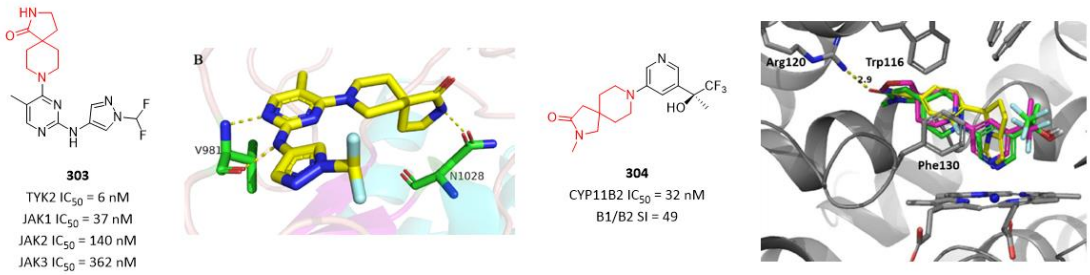

Figure 94. Spirocyclic amides used in discovery of selective inhibitors

In above case stories, spirocyclic amide building blocks played critical roles in quick access of designed molecules and SAR/SPR data (**Figure 95**). Oxygen of carbonyl of lactam can be a strong hydrogen bond acceptor, while NH of lactam can be a strong hydrogen bond donor.

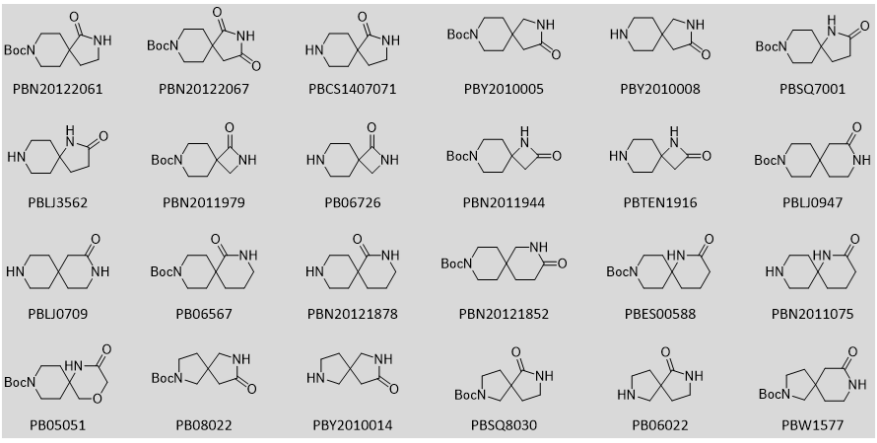

Figure 95. Spirocyclic amide building blocks

In **Figure 96**, a variety of spirocyclic rings were explored in discovery of JAK1 selective inhibitors, and resulted in identification of clinical candidate **306** based on **Filgotinib** (**305**) approved as a JAK1

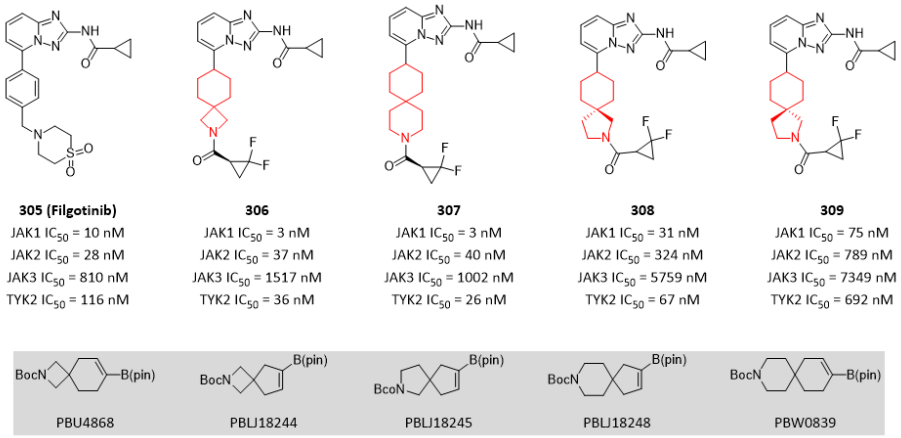

Figure 96. Spirocyclic rings used in discovery of selective JAK1 inhibitors

inhibitor for treatment of autoimmune and inflammatory diseases. Both compound **306** and compound **307** showed excellent JAK1 inhibition and selectivity against other JAK family members. In compound **308** and compound **309**, JAK1 inhibition was decreased by > 10-fold, most likely due to unfavored geometry of the molecule for JAK binding (**Figure 96**). [21]

References

[1] Kerstin Hiesinger; *et al.* Spirocyclic scaffolds in medicinal chemistry. *J. Med. Chem.* **2021**, *64*, 150-183.

[2] Oleksandr O. Grygorenko; *et al.* Bicyclic conformationally restricted diamines. *Chem. Rev.* **2011**, *111*, 5506-5568.

[3] Nicholas A. Meanwell; *et al.* Applications of isosteres of piperazine in the design of biologically active compounds: part 1. *J. Agric. Food Chem.* **2022**, *70*, 10942-10971.

[4] Sebastien L. Degorce; *et al.* Lowering lipophilicity by adding carbon: azaspiroheptanes, a logD lowering twist. *ACS Med. Chem. Lett.* **2019**, *10*, 1198-1204.

[5] Ilaria Proietti Silvestri; *et al.* The growing importance of chirality in 3D chemical space exploration and modern drug discovery approaches for hit-ID. *ACS Med. Chem. Lett.* **2021**, *12*, 1220-1229.
[6] Satoru Noji; *et al.* Discovery of a Janus kinase inhibitor bearing a highly three-dimensional spiro scaffold: JTE-052 (Delgocitinib) as a new dermatological agent to treat inflammatory skin disorders. *J. Med. Chem.* **2020**, *63*, 7163-7185.
[7] Edwige Lorthiois; *et al.* JDQ443, a structurally novel, pyrazole-based, covalent inhibitor of KRAS G12C for the treatment of solid tumors. *J. Med. Chem.* **2022**, *65*, 16173-16203.
[8] Victor S. Gehling; *et al.* Design and synthesis of styrenylcyclopropylamine LSD1 inhibitors. *ACS Med. Chem. Lett.* **2020**, *11*, 1213-1220.
[9] Manjiong Wang; *et al.* Drug repurposing of Quisinostat to discover novel Plasmodium falciparum HDAC1 inhibitors with enhanced triple-stage antimalarial activity and improved safety. *J. Med. Chem.* **2022**, *65*, 4156-4181.
[10] Sean W. Reilly; *et al.* Examination of diazaspiro cores as piperazine bioisosteres in the Olaparib framework shows reduced DNA damage and cytotoxicity. *J. Med. Chem.* **2018**, *61*, 5367-5379.
[11] Sean W. Reilly; *et al.* Highly selective dopamine D3 receptor antagonists with arylated diazaspiro alkane cores. *J. Med. Chem.* **2017**, *60*, 9905-9910.
[12] Yasuko Koda; *et al.* Design and synthesis of tranylcypromine-derived LSD1 inhibitors with improved hERG and microsomal stability profiles. *ACS Med. Chem. Lett.* **2022**, *13*, 848-854.
[13] Patrick Sarver; *et al.* 6-Amino-3-methylpyrimidinones as potent, selective, and orally efficacious SHP2 inhibitors. *J. Med. Chem.* **2019**, *62*, 1793-1802.
[14] Bagdanoff J. T.; *et al.* Optimization of fused bicyclic allosteric SHP2 inhibitors. *J. Med. Chem.* **2019**, *62*, 1781-1792.
[15] Anders Johansson; *et al.* Discovery of (3-(4-(2-oxa-6-azaspiro[3.3]heptan-6-ylmethyl)phenoxy) azetidin-1-yl)(5-(4-methoxyphenyl)-1,3,4-oxadiazol-2-yl)methanone (AZD1979), a melanin concentrating hormone receptor 1 (MCHr1) antagonist with favorable physicochemical properties. *J. Med. Chem.* **2016**, *59*, 2497-2511.
[16] Caroline Wilson; *et al.* Optimization of TAM16, a benzofuran that inhibits the thioesterase activity of Pks13; evaluation toward a preclinical candidate for a novel antituberculosis clinical target. *J. Med. Chem.* **2022**, *65*, 409-423.
[17] Tim Cernak; *et al.* Microscale high-throughput experimentation as an enabling technology in drug discovery: application in the discovery of (piperidinyl)pyridinyl-1H-benzimidazole diacylglycerol acyltransferase 1 inhibitors. *J. Med. Chem.* **2017**, *60*, 3594-3605.
[18] Aurelie Mallinger; *at al.* Discovery of potent, orally bioavailable, small-molecule inhibitors of WNT signaling from a cell-based pathway screen. *J. Med. Chem.* **2015**, *58*, 1717-1735.
[19] Tao Yang; *et al.* Identification of a novel 2,8-diazaspiro[4.5]decan-1-one derivative as a potent and selective dual TYK2/JAK1 inhibitor for the treatment of inflammatory bowel disease. *J. Med. Chem.* **2022**, *65*, 3151-3172.
[20] Whitney L. Petrilli; *et al.* Discovery of spirocyclic aldosterone synthase inhibitors as potential treatments for resistant hypertension. *ACS Med. Chem. Lett.* **2017**, *8*, 128-132.
[21] Shuhao Zhou; *et al.* Identification of TUL01101: a novel potent and selective JAK1 inhibitor for the treatment of rheumatoid arthritis. *J. Med. Chem.* **2022**, *65*, 16716-16740.

Fused Cyclic Rings in Medicinal Chemistry

There are three types of bicyclic aliphatic rings: spirocyclic, fused cyclic and bridged cyclic, all of which have been gaining substantial interest in medicinal chemistry. [1-3] Like spirocyclic rings, fused cyclic ring system is also one of the most popular strategies of modern medicinal chemistry, as can be seen by the number of publications and contributions to a variety of approved drugs and clinical candidates (**Figure 97**). The increase in rigidity resulting from fused cyclization can influence important factors, such as potency and selectivity. Furthermore, significant improvements in physicochemical properties, such as logD, lipophilicity and solubility, as well as ADMET properties, are achievable, ultimately leading to improved pharmacokinetic profiles. Recent advances in the development of synthetic methods and efficient supplies of diverse **fused cyclic building blocks** have allowed the introduction and increase in fused cycles in medicinal chemistry in the past decade.

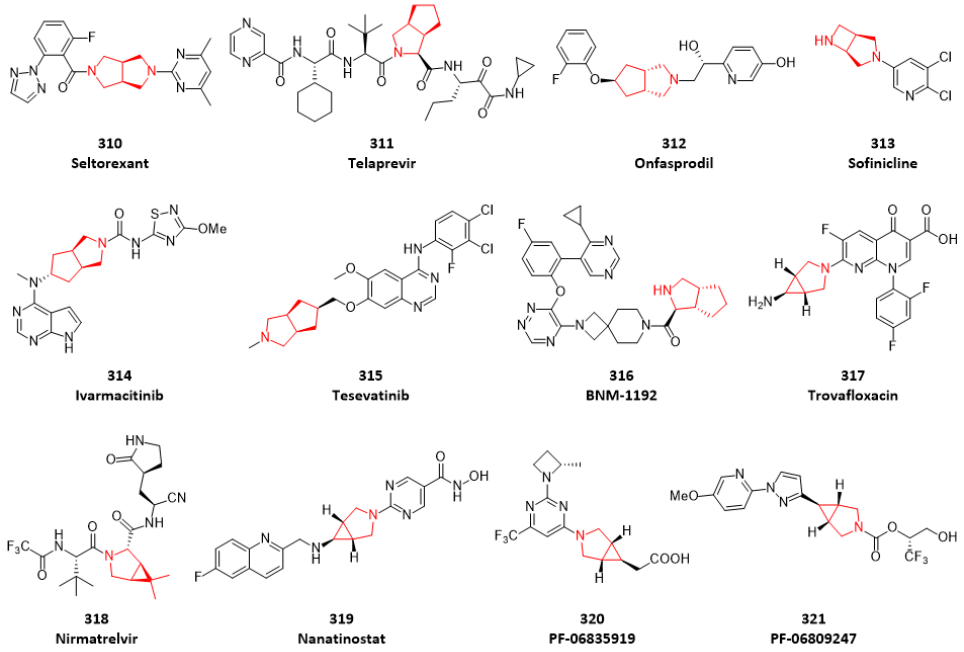

Figure 97. Fused cyclic rings in drug or clinical candidate molecules

In order to discover novel KHK inhibitors, compound **322** was identified as a promising hit. X-ray structure of compound **322** bound to KHK protein revealed that the cis-dihydroxypyrrolidine substituent is in line with the Arg108 residue at the polar back portion of the ATP binding site normally occupied by the triphosphate side chain in KHK. The team sought to exploit this vector in the direction of Arg108 in an effort to improve potency, possibly utilizing a Coulombic interaction. Additionally, a HydroSite calculation predicted a high-energy virtual water molecule in this pocket present within the hydrogen-bonding distance between Arg108, a backbone carbonyl oxygen atom of Thr253, and a backbone NH of Gly257 respectively, suggesting the possibility of making energetically favorable interactions with an appropriately chosen side chain attachment in this regioin. With this in mind, initial exploration of this vector by parallel medicinal chemistry using a diverse array of amines culminated in the identification of compound **323**, possessing a fused cyclic 3-azabicyclo[3.1.0]hexane ring system as one of the most potent neutral azetidine analogues among those tested from parallel medicinal chemistry effort (**Figure 98**). [4] X-ray structure of compound **323** bound in KHK protein showed that the terminal hydroxyl group on the newly

introduced 3-azabicyclo[3.1.0]hexane ring system effectively reached proximally to Arg108. This terminal hydroxyl group indirectly forms a hydrogen bond with Arg108 through a bound water, while within the hydrogen bond distance with the backbone carbonyl oxygen atom of Thr253. With compound **323** in hand, further optimization of the terminal polar groups was targeted as next design strategy to improve potency. Among the polar group known to interact with the arginine residue, the carboxylic acid group was considered as one of the top candidates given its potential to form a strong salt bridge with the guanidinium group of Arg108. This was proved by compound **324**, which demonstrated significantly increased potency by > 20-fold compared to compound **323**. X-ray structure of compound **324** bound to KHK protein displayed that the carboxylic acid group was well positioned to interact with cationic guanidinium group of Arg108. In addition, the backbone NH of Gly255 and Gly257, as well as a bound water nearby, were all within the hydrogen bond distance. Thus, a complex network of polar interactions through the carboxylic acid is likely responsible for the significant potency improvement. Further optimization based on compound **324** led to identification of clinical candidate **PF-06835919** (compound **320**).

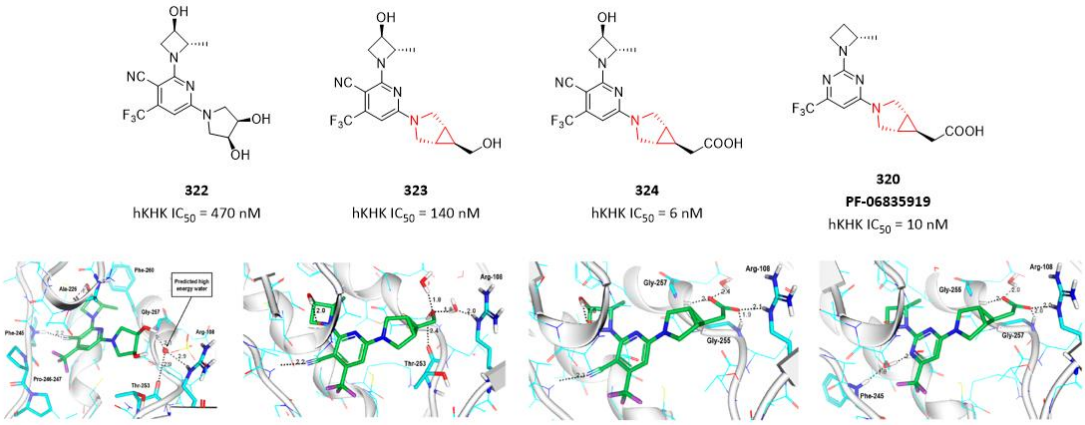

Figure 98. Fused 3-azabicyclo[3.1.0]hexane ring in KHK inhibitors (PDB codes: 6W0W, 6W0X, 6W0Y, 6W0Z)

In the course of discovery of MAGL inhibitor **PF-06795071** (compound **321**), the team previously identified a series of azetidine analogs such as compound **325**, which displayed excellent MAGL potency with IC_{50} = 0.3 nM and a good selectivity profile. However, in vivo PK-PD studies, only a transient elevation in 2-AG was observed. Cellular activity based protein profiling studies confirmed that this class of compounds covalently inhibited MAGL transiently and led the team to speculate that the azetidine adducts formed at the MAGL site were rapidly hydrolyzed from the enzyme. With an observation in mind that analogs containing larger ring cores, such as piperidines, resulted in improved MAGL adduct stability and thus prolonged PD effects, efforts to optimize the core system resulted in the discovery of compounds based on 3-azabicyclo[3.1.0]hexane ring system, such as compound **326**. Compound **326** retained MAGL potency with IC_{50} = 1.4 nM and had excellent selectivity. Despite a promising pharmacology profile, compound **326** had poor solubility (< 1 uM). To address this issue, the team systematically explored leaving group with the goal of improving drug-like properties, which led to discovery of clinical candidate **PF-06809247** (compound **321**) with significantly increased solubility. X-ray structure of compound **326** bound to MAGL protein revealed that 3-azabicyclo[3.1.0]hexane core with aryl pyrazole tail complements the shape of the lipophilic MAGL acyl chain binding pocket (**Figure 99**). [5]

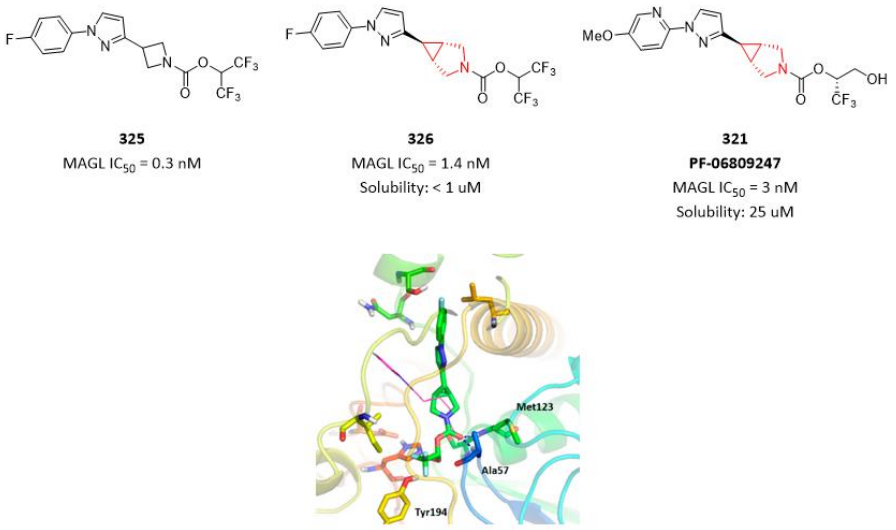

Figure 99. Fused 3-azabicyclo[3.1.0]hexane ring in MAGL inhibitors (PDB codes: 6BQ0)

PBTZ169 (compound **327**) is a promising compound which possesses extraordinary while-cell activity with a minimum inhibitory concentration (MIC) of 1 nM. While impressive, **PBTZ169** has liabilities emanating from its extremely poor solubility (< 0.01 ug/mL) that portend poor penetration. This may affect oral bioavailability (F) and volume of distribution (V_d), neither of which have been reported. To address this issue, disruption of molecular symmetry and planarity was used to improve aqueous solubility by replacing piperazine moiety with a wide variety of bioisosteric spirocyclic, fused cyclic and bridged cyclic diamines. This effort led to identification of compound **328** and compound **329** which possess a bridged cyclic ring and a fused cyclic ring respectively. Both compounds had high potency with MIC_{90} = 32 nM, although 15-fold less potent than **PBTZ169**. Fused 3-azabicyclo[3.1.0]hexane ring in compound **329** significantly increased aqueous solubility by at least 480-fold, while metabolic stability in both human and mouse liver microsome were both improved. However, compound **328** failed to improve solubility, and had a similar metabolic stability profile with **PBTZ169** (**Figure 100**). [6]

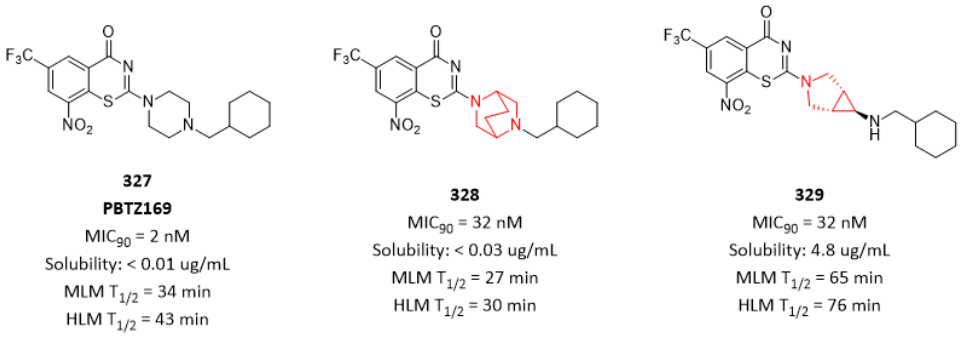

Figure 100. Fused 3-azabicyclo[3.1.0]hexane ring improved both solubility and metabolic stability.

To identify new potent and selective allosteric SHP2 inhibitors, the team led to discovery of a promising hit compound **330**, which exhibited modest SHP2 inhibition with IC_{50} = 225 nM. An attempt to optimize the novel amino moiety was undertaken with objectives: (a) maximize SHP2 inhibition; (b) remove secondary amine groups which are potentially detrimental to cell penetration; (c) make molecule constrained to likely control metabolic stability. With these goals in mind, a variety of fused cyclic diamines were examined and these efforts led to identification of compound **331** which possesses a bicyclo[3.1.0]hexane ring. Compound **331** had an excellent SHP2

inhibition with IC_{50} = 9 nM, and a modest pERK inhibition with IC_{50} = 210 nM. In order to further increase potency, a bicyclic pyrazopyrazole scaffold in compound **332** was employed with pERK inhibition increased by up to 10-fold. Despite promising in vitro potency, compound **332** inhibited hERG with IC_{50} = 58 nM. In order to address this critical issue, dichlorophenyl group was replaced by various bicyclic heterocycles. Among of them, indazole in compound **333** was found to decrease hERG inhibition while keeping excellent in vitro potency. Surprisingly, the corresponding 3-azabicyclo[3.1.0]hexane ring in compound **334** showed excellent in vitro potency and significantly lower hERG inhibition (**Figure 101**). [7]

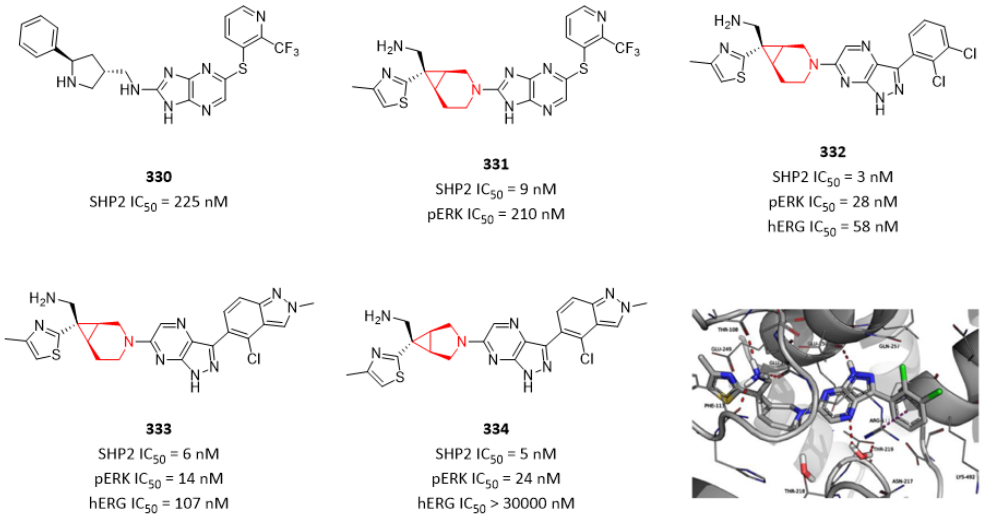

Figure 101. Fused 3-azabicyclo[3.1.0]hexane ring decreased hERG inhibition. (PDB code: 8CBH)

As can be seen in above case stories, a quick access of a diverse collection of fused cyclic building blocks is of great value for medicinal chemists to get SAR or SPR results in their program as soon as possible (**Figure 102**).

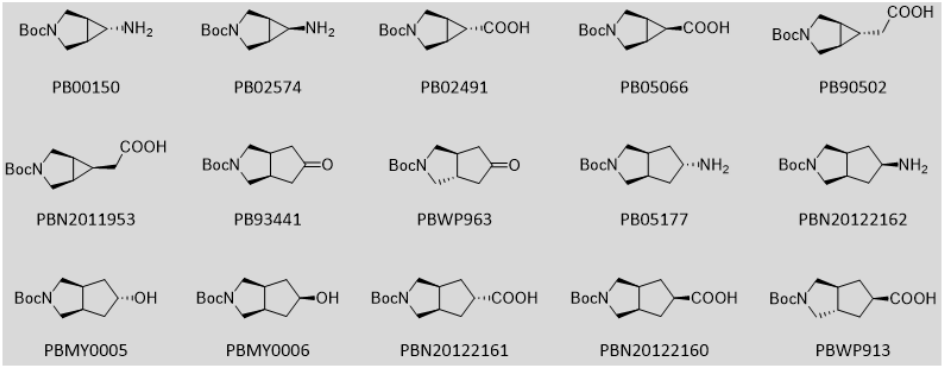

Figure 102. Fused cyclic building blocks with different functional groups

Discovery of compound **339** (**SAR707**) was started from reported compound **335**. Replacement of piperazine moiety with fused hexahydro-pyrrolo-pyrrole ring in compound **336** increased potency by 5-fold. SAR study around the left chain identified compound **337** as the most potent compound, which possesses a cyclopropane. Replacing pyridine with pyridazine in compound **338** didn't change potency. Surprisingly, in compound **339** (**SAR707**), phenyl ring increased SCD1 potency significantly by 25-fold (**Figure 103**). [8]

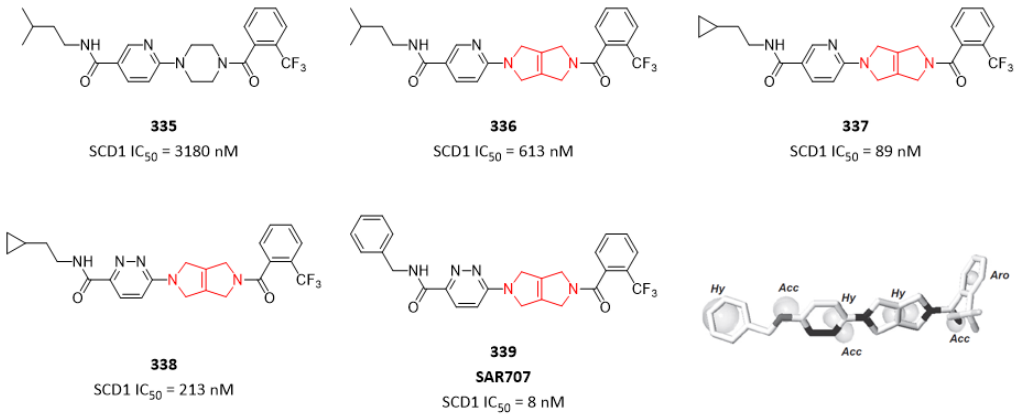

Figure 103. Fused hexahydro-pyrrolo-pyrrole ring in discovery of **SAR707**.

Compound **341** was discovered through an optimization program based on hit compound **340**, and potency was increased by 7-fold. However, compound **341** had CYP inhibition with IC_{50} = 7 uM for CYP3A4 and IC_{50} = 12 uM for CYP2D6 respectively. In order to address this critical issue, replacing piperazine with bioisosteres was employed. One piperazine isostere of interest was the fused octahydropyrrolo[3,4-c]pyrrole ring. As showed in compound **342**, fused octahydropyrrolo[3,4-c]pyrrole also increased potency by 7-fold, but still had CYP inhibition with IC_{50} = 6 uM for CYP3A4 and IC_{50} = 24 uM for CYP2D6 respectively. Further optimization led to compound **343** where adamantly group was replaced with a spirocyclic ring, which demonstrated no CYP3A4 and CYP2D6 inhibition (**Figure 104**). [9]

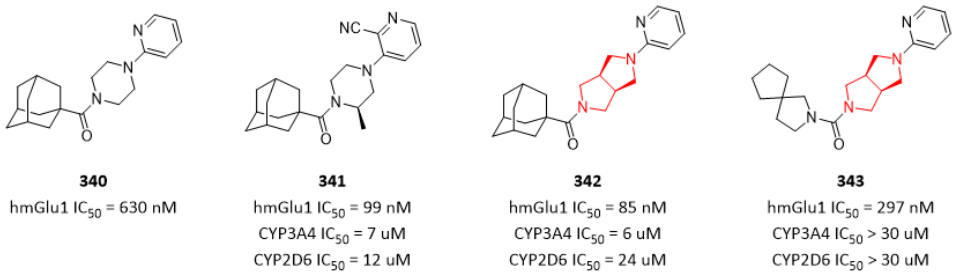

Figure 104. Fused octahydropyrrolo[3,4-c]pyrrole ring increased potency.

In order to discover novel, selective OX2R antagonists that were orally bioavailable and safe with an optimal pharmacokinetic profile for the treatment of primary insomnia, a high-throughput screening campaign was conducted identified a promising hit compound **344**. To further optimize compound **344**, the team decided to investigate SAR and selectivity of compounds with novel core structures. These efforts generated compound **345** possessing a fused octahydropyrrolo[3,4-c]pyrrole ring, which decreased potency significantly by 88-fold. Despite low potency, iterative SAR led to great improvements in both OX2R affinity and selectivity against OX1R, and culminated in discovery of clinical candidate **Seltorexant** (compound **310**) (**Figure 105**). [10]

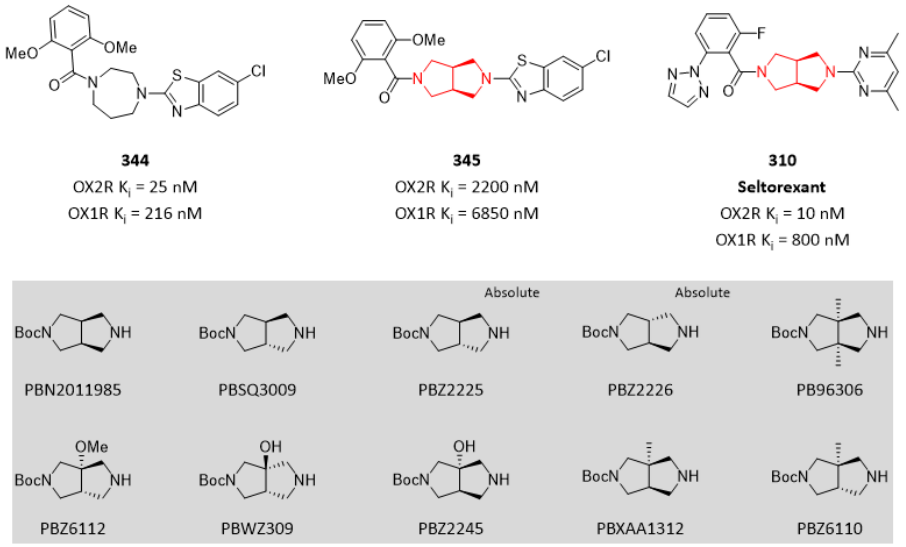

Figure 105. Fused octahydropyrrolo[3,4-c]pyrrole ring in selective OX2R antagonists

To optimize compound **346**, a series of potent neuronal nAChR ligands based on fused 3,8-diazabicylco[4.2.0]octane ring have been synthesized and evaluated for affinity and agonist efficacy at human high affinity nicotine recognition site and in a rat model of persistent nociceptive pain. Among of them, compound **347** and compound **348** exhibited equivalent or greater affinity relative to epibatidine, and demonstrated robust analgesic efficacy in the rat formalin model of persistent pain (**Figure 106**). [11] Fused 3,8-diazabicylco[4.2.0]octane ring was also used in discovery of novel dual orexin receptor antagonists via scaffold hopping approach based on compound **349** (**Suvorexant**). Compound **350** displayed comparable potency to compound **349** (**Suvorexant**). [12]

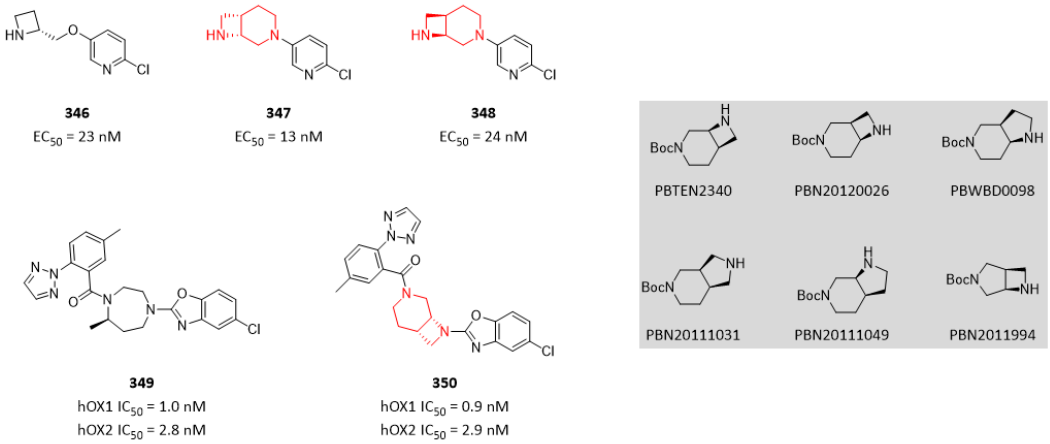

Figure 106. Fused 3,8-diazabicylco[4.2.0]octane ring used in drug discovery

Fused cyclic diamines have been widely used in discovery of novel antibacterial drugs. Based on compound **351**, an additional ring was formed to generate compound **352** which increased potency by 7-fold. However, compound **352** inhibited hERG with 36% inhibition at 100 uM. To address this critical issue, a polar oxygen atom was inserted in compound **353**, and interestingly hERG inhibition was not observed (**Figure 107**). [13] In another work, compound **354** was identified as a highly potent antibacterial inhibitor. Further optimization by introduction of a fused cyclic ring and two fluorine atoms, led to discovery of compound **355** which significantly increased antibacterial potency by 33-

fold. Furthermore, compound **355** also decreased *in vivo* clearance and increased *in vivo* exposure and oral bioavailability. [14]

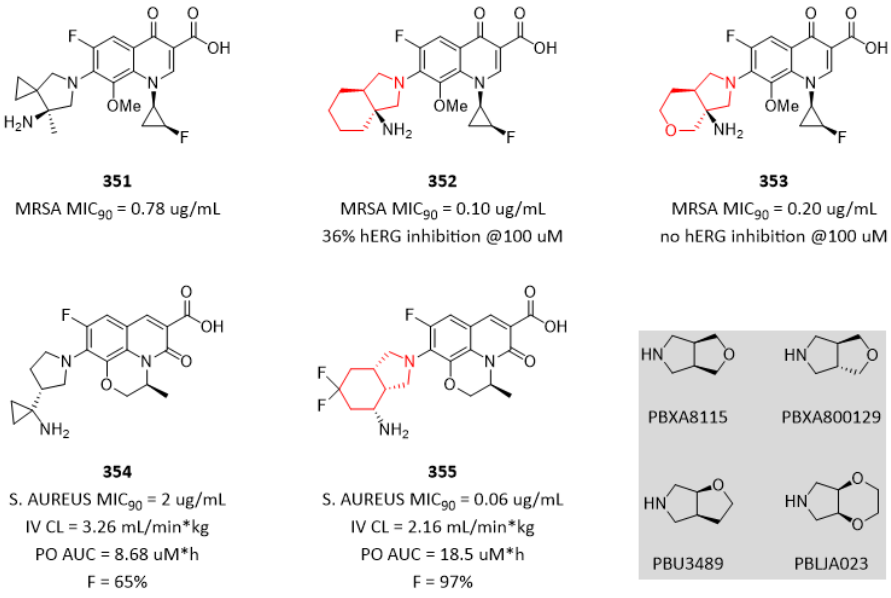

Figure 107. Fused cyclic rings used in discovery of novel antibacterial drugs

The fusion of a cyclopropane ring with two of the carbon of piperazine reduces the basicity of the nitrogen atom. This is attributed to a combination of the known effect of the cyclopropane ring on amine basicity which typically reduces pKa values by 1.15 units, coupled with an effect resulting from the two nitrogen atoms being slightly closer in proximity, disposing at a distance of 2.77 A compared to 2.86 A in the piperazine. The ring fusion also confers an element of conformational constraint. In an effort to assess the potential fused 2,5-diazabicyclo[4.1.0]heptane ring to substitute for the C-7 piperazine ring of compound **356**, analogue **357** was synthesized and evaluated for its in vitro antibacterial properties. The antibacterial potency of compound **357** was comparable to that of compound **356**. In the single crystal X-ray structure of compound **357**, the fused 2,5-diazabicyclo[4.1.0]heptane ring exists in a twist boat-like conformation that results in some distortion of cyclopropane ring (**Figure 108**). [15]

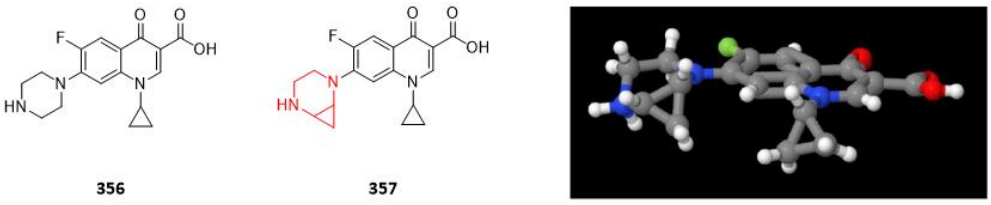

Figure 108. Conformation of fused 2,5-diazabicyclo[4.1.0]heptane ring

It would be greatly interesting to investigate conformation and impact on biological activity of other fused piperazine rings. An efficient access of this kind of building blocks can provide us more insights in potential applications in drug discovery (**Figure 109**).

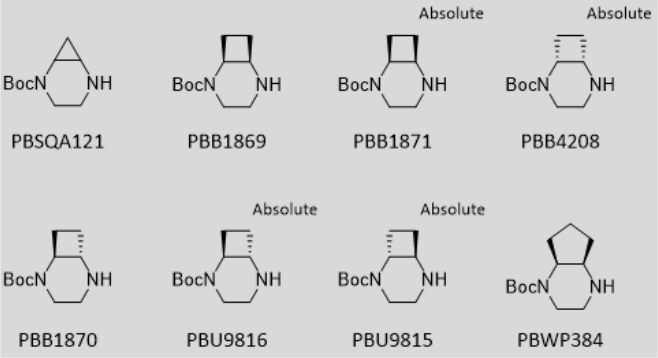

Figure 109. Fused piperazine building blocks

In the course of discovery of clinical candidate **NTQ1062** (compound **359**) as an AKT inhibitor, it was surprisingly to found that the inhibitory of fused piperazine compound **359** was improved by 4-fold compared with compound **358**, and more importantly the exposure was increased by 9-fold. The predicted binding model of compound **359** revealed that the distance between the sulfur in the amino acid residue of Met281 and the cyclopropyl was 3.6 A. The cyclopropyl ring has properties similar to those of carbon-carbon double bond of alkene. Therefore, it was speculated that additional sulfur-pi interaction might contribute to the increase in the potency of compound **359** (**Figure 110**). [16]

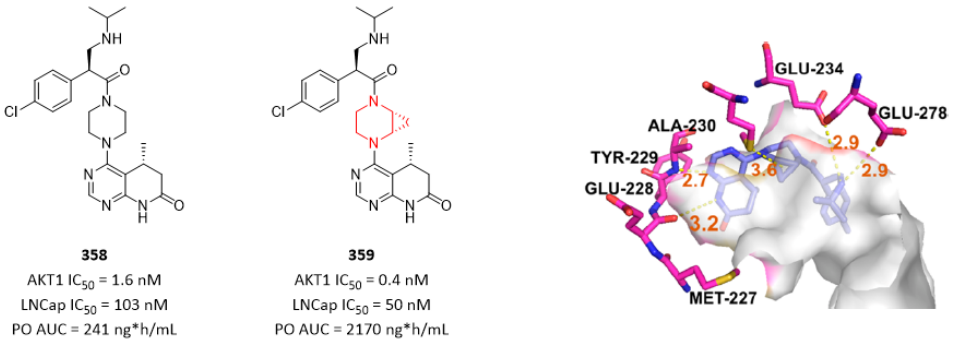

Figure 110. Fused piperazine increased both potency and exposure.

References

[1] Oleksandr O. Grygorenko; *et al.* Bicyclic conformationally restricted diamines. *Chem. Rev.* **2011**, *111*, 5506-5568.
[2] Nicholas A. Meanwell; *et al.* Applications of isosteres of piperazine in the design of biologically active compounds: part 1. *J. Agric. Food Chem.* **2022**, *70*, 10942-10971.
[3] Nicholas A. Meanwell; *et al.* Applications of isosteres of piperazine in the design of biologically active compounds: part 1. *J. Agric. Food Chem.* **2022**, *70*, 10972-11004.
[4] Kentaro Futatsugi; *et al.* Discovery of PF-06835919: a potent inhibitor of ketohexokinase (KHK) for the treatment of metabolic disorders driven by the overconsumption of fructose. *J. Med. Chem.* **2020**, *63*, 13546-13560.
[5] Laura A. McAllister; *et al.* Discovery of trifluoromethyl glycol carbamates as potent and selective covalent monoacylglycerol lipase (MAGL) inhibitors for treatment of neuroinflammation. *J. Med. Chem.* **2018**, *61*, 3008-3026.
[6] Gang Zhang; *et al.* Spirocyclic and bicyclic 8-nitrobenzothiazinones for tuberculosis with improved physicochemical and pharmacokinetic properties. *J. Med. Chem.* **2019**, *10*, 348-351.

[7] Alessia Petrocchi; *et al.* Discovery of a novel series of potent SHP2 allosteric inhibitors. *ACS Med. Chem. Lett.* **2023**, *14*, 645-651.
[8] Marc D. Voss; *et al.* Discovery and pharmacological characterization of SAR707 as novel and selective small molecule inhibitor of stearoyl-CoA desaturase (SCD1). *Eur. J. Pharmacol.* **2013**, *707*, 140-146.
[9] Jason T. Manka; *et al.* Octahydropyrrolo[3,4-c]pyrrole negative allosteric modulators of mGlu1. *Bioorg. Med. Chem. Lett.* **2013**, *18*, 5091-5096.
[10] Michael A. Letavic; *et al.* Novel octahydropyrrolo[3,4-c]pyrroles are selective orexin-2 antagonists: SAR leading to a clinical candidate. *J. Med. Chem.* **2015**, *58*, 5620-5636.
[11] Jennifer M. Frost; *et al.* Synthesis and structure-activity relationships of 3,8-diazabicyclo[4.2.0]octane ligands, potent nicotinic acetylcholine receptor agonists. *J. Med. Chem.* **2006**, *49*, 7843-7853.
[12] Bibia Heidmann; *et al.* Discovery of highly potent dual orexin receptor antagonists via a scaffold-hopping approach. *ChemMedChem* **2016**, *11*, 1-16.
[13] Takashi Odagiri; *et al.* Design, synthesis, and biological evaluation of novel 7-[(3aS,7aS)-3a-aminohexahydropyrano[3,4-c]pyrrol-2(3H)-yl]-8-methoxyquinolines with potent antibacterial activity against respiratory pathogens. *J. Med. Chem.* **2018**, *61*, 7234-7244.
[14] Guillaume Lapointe; *et al.* Discovery and optimization of DNA gyrase and topoisomerase IV inhibitors with potent activity against fluoroquinolone-resistant gram-positive bacteria. *J. Med. Chem.* **2021**, *64*, 6329-6357.
[15] Taylor R. R. R.; *et al.* Substituted 2,5-diazabicyclo[4.1.0]heptanes and their application as general piperazine surrogates: synthesis and biological activity of a ciprofloxacin analogue. *Tetrahedron* **2010**, *66*, 3370-3377.
[16] Changyou Ma; *et al.* Discovery of clinical candidate NTQ1062 as a potent and bioavailable Akt inhibitor for the treatment of human tumors. *J. Med. Chem.* **2022**, *65*, 8144-8168.

Bridged Cyclic Rings in Medicinal Chemistry

Like spirocyclic rings and fused cyclic rings, bridged cyclic ring system is also one of the most popular focus of modern medicinal chemistry, as can be seen by a wide range of applications of bridged cyclic rings in approved drug and clinical candidate molecules (**Figure 111**).

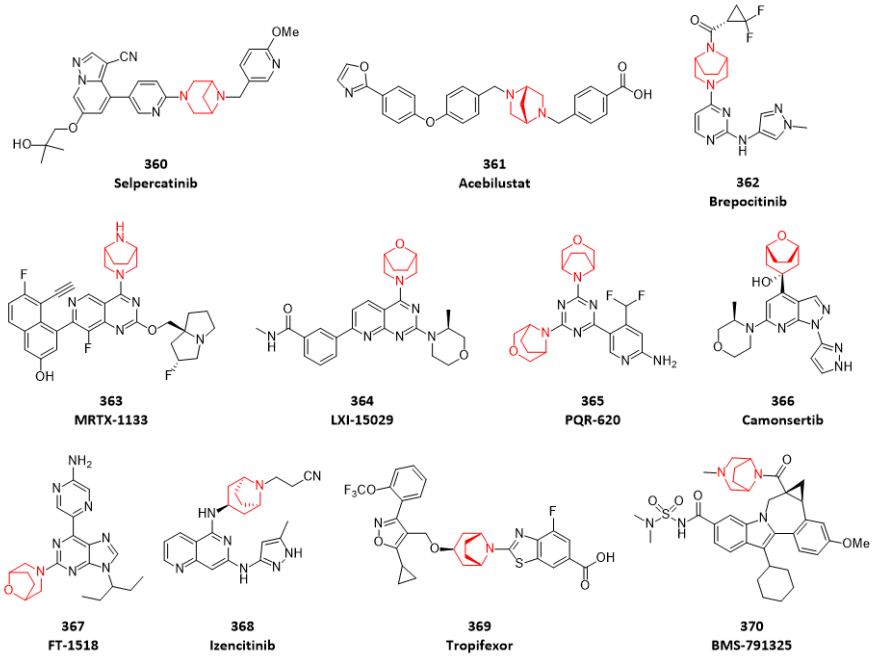

Figure 111. Approved drug and clinical candidate molecules containing bridged cyclic rings

Bridging piperazines, piperidines, morpholines and other mono-rings with one, two or even more carbon atoms can confer them with unexpected observations due to conformational restrictions (**Figure 112**). For instance, it was recommended that medicinal chemists consider the use of one-carbon bridges as a potential strategy to modulate the physicochemical properties of morpholines and piperazines, especially in cases where issues are observed with metabolism, hERG inhibition, or other detrimental properties correlated with lipophilicity. In addition, specific benefits, particularly where the conformational restrictions can potentially be used to improve selectivity or increase potency via subtly changing the shape of the moiety. [1]

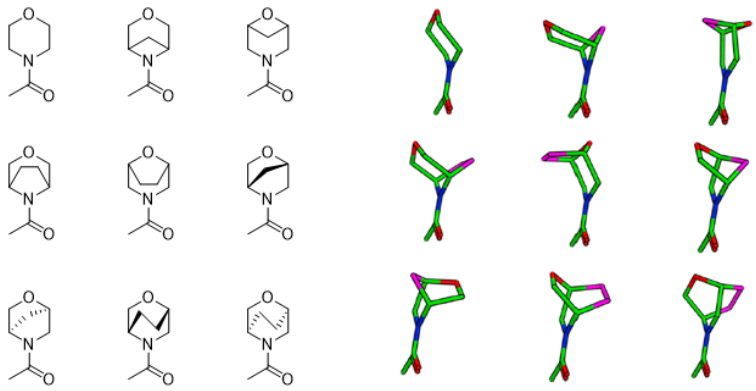

Figure 112. 3-D models of various bridged N-acetylmorpholines (bridged carbons are shown in purple)

In the course of discovery of clinical candidate **Brepocitinib** (compound **362**), a variety of bridged rings were examined in compound **371**, **372**, **373**, **374**, **375**, **376** and **362**. A clear stereochemical

preference is evident from the biochemical activity of compound **371** and compound **372**. Potency against TYK2 improved for compound **374**, compound **375** and compound **376** compared to compound **373**, presumably due to improved hydrophobic interactions of bridged carbon atoms with the residues at the bottom of the binding site. Among of these compounds, compound **376** containing 3,8-diazabicyclo[3.2.1]octane ring demonstrated the highest potency. Further optimization led to discovery of clinical candidate **Brepocitinib** (compound **362**). To better understand the TYK2 potency, a crystal structure of compound **362** bound to TYK2 was obtained. The ethylene bridge of the [3.2.1]-diazabicycle projects into the lower hydrophobic portion of the binding site (**Figure 113**). [2]

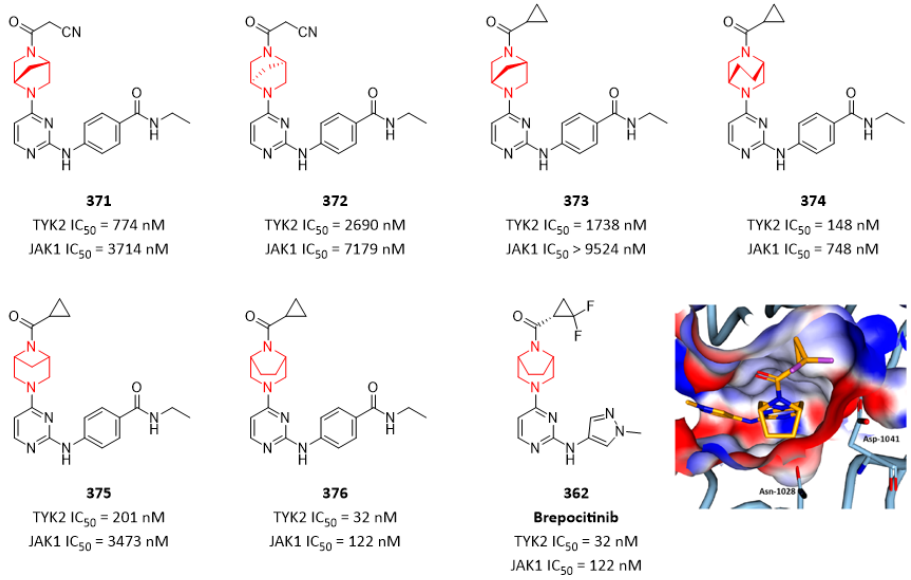

Figure 113. Bridged cyclic rings used in discovery of **Brepocitinib** (PDB code: 6DBM)

As described in above case story, an efficient access of diverse **bridged piperazine building blocks** is of great value for quick exploration of SAR and SPR (**Figure 114**).

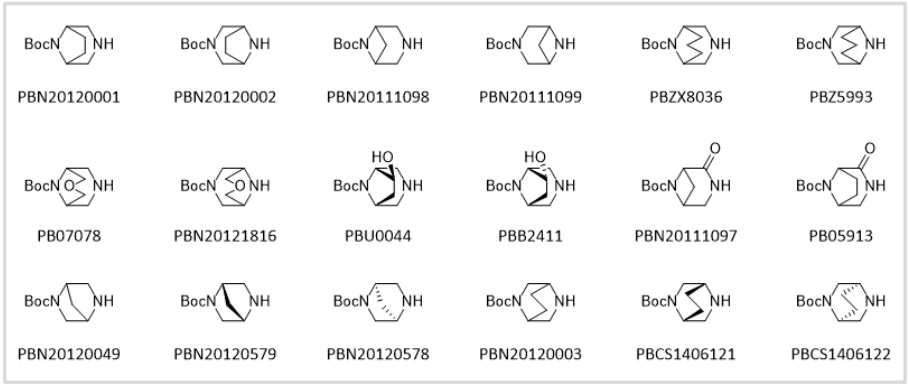

Figure 114. Bridged piperazine building blocks

In order to discover novel KRAS G12D inhibitor, like discovery of **Brepocitinib** (compound **362**) in above, a variety of bridged rings were examined in compound **378**, **379**, **380**, **381**, and **363**. Comparing with compound **377**, all rigidification of bioactive conformation with bridged piperazine increased affinity. Among of them, compound **381** containing a [3.2.1]bicyclic diamino substituent had a 200-fold greater affinity than compound **377**. The X-ray structure of compound **381** bound to KRAS G12D revealed that two-carbon bridge of the bicyclic group occupies a small pocket, while

one of the endo C-Hs forms a non-classical hydrogen bond with the Gly10 carbonyl oxygen (**Figure115**). [3]

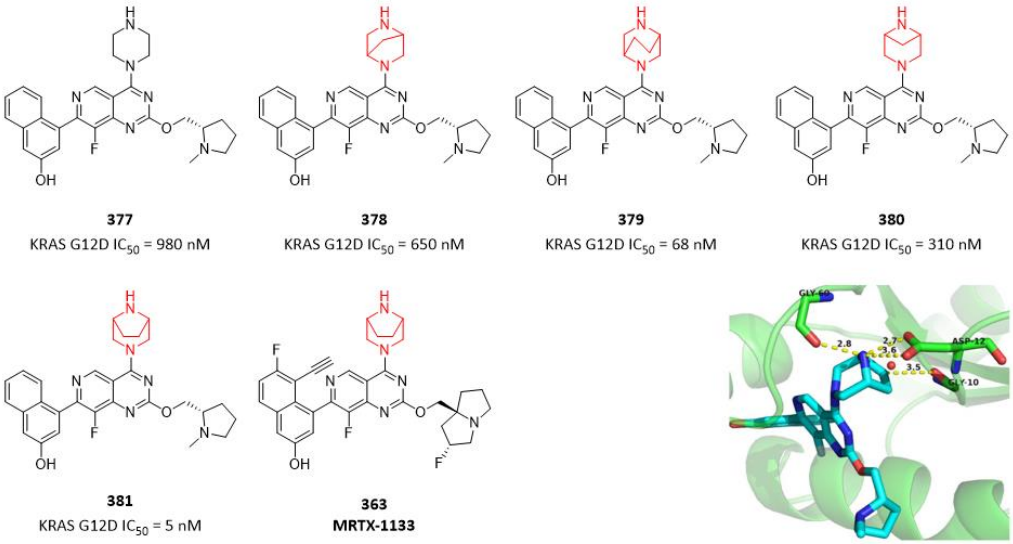

Figure 115. Bridged cyclic rings used in discovery of **MRTX-1133** (PDB code: 7RT1)

In the last section "**Fused Cyclic Rings in Medicinal Chemistry**", we described further optimization of compound **358** which suffered poor oral exposure. Besides fused cyclic rings, the team also investigated bridged cyclic piperazines for improving oral exposure. As shown in compound **382** and compound **383**, 3,8-diazabicyclo[3.2.1]octane ring increased oral exposure by 4-fold and 6-fold respectively (**Figure 116**). However, compound **383** decreased cellular potency by 4-fold. [4]

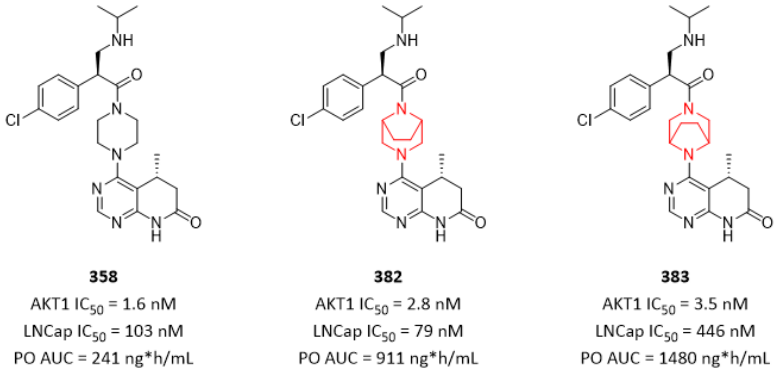

Figure 116. Bridged rings increased oral exposure.

In the course of discovery of clinical candidate **BMS-791325** (compound **370**) as a potent allosteric inhibitor of the hepatitis C virus NS5B polymerase, a variety of bridged cyclic rings were examined to address off-target activities, most notably hPXR transactivation which led to identification of compound **384**. Compound **384**, containing a 3,6-diazabicyclo[3.1.1]heptane ring, had a highly potency and no hPXR issue, but inhibited CYP3A4 with IC_{50} = 14 uM. It was interesting that in compound **370** (**BMS-791325**), containing a 3,8-diazabicyclo[3.2.1]octane ring, demonstrated no CYP3A4 inhibition (**Figure 117**). [5] X-ray structure of compound **370** bound in NS5B revealed that additional contacts between two-carbon bridge of the bicyclic group and proximal protein residues L492, T399 and A400 were observed.

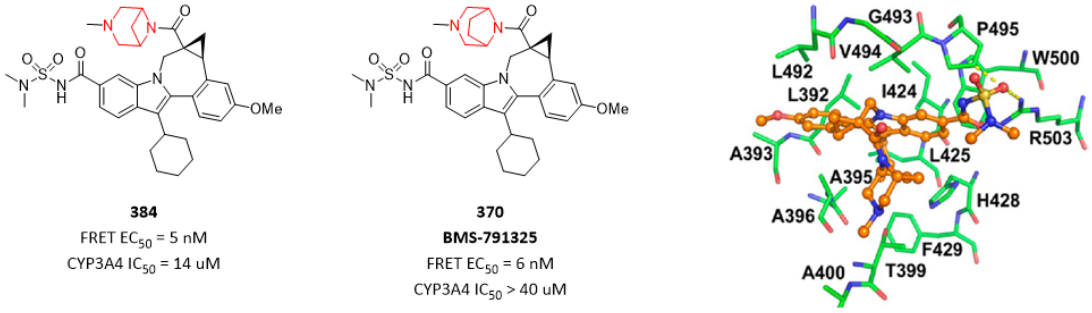

Figure 117. 3,8-Diazabicyclo[3.2.1]octane ring address CYP3A4 inhibition.

Compound **385** was identified as a potent, brain-penetrant and selective M1R antagonist, but showed low metabolic stability and inhibition against hERG. To address these issues, many bridged cyclic rings in compound **386** (**PIPE-359**), compound **387** and compound **388** were examined. A 3,8-diazabicyclo[3.2.1]octane ring in compound **386** (**PIPE-359**) not only increased activity, but also improved metabolic stability and hERG inhibition. However, in compound **387** and compound **388**, two bridged cyclic rings displayed inferior activity (**Figure 118**). [6]

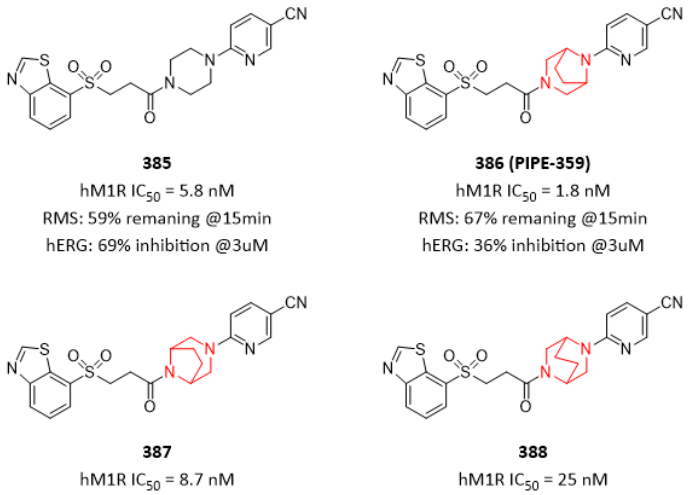

Figure 118. 3,8-Diazabicyclo[3.2.1]octane ring address metabolic stability and hERG inhibition issues.

In order to discover FGFR2 and FGFR3 dual inhibitors with high selectivity against FGFR1 and FGFR4, compound **389** was selected as starting point. Encouraged by previous work, piperazine bearing 2,6-dimethyl group displayed improved FGFR3 potency in comparison to unsubstituted piperazine, suggesting an opportunity to enhance potency and selectivity by introduction of carbon bridge on piperazinone ring. Pleasingly, compound **390**, featuring an ethylene bridge between C-2 and C-6 of the piperazinone, displayed single-digit-nanomolar potency against FGFR3 while maintaining good selectivity against FGFR1 (16-fold). Further optimization led to identification of more promising compound **391**. Docking of compound **391** in binding site revealed that the bridged piperazinone occupies the pocket under the P loop, wherein the ethylene bridge is oriented toward a hydrophobic groove formed by Leu624 and Ala634, placing the amide carbonyl group in the proper position to form a strong hydrogen bond with the catalytic Lys508 (**Figure 119**). [7]

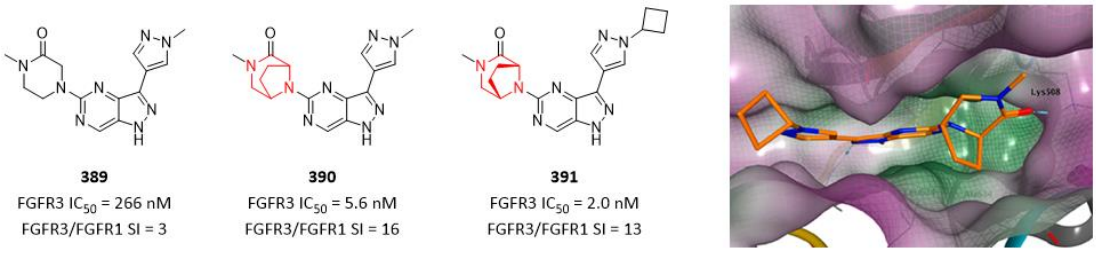

Figure 119. Bridged piperazinone increased both potency and selectivity.

In the course of discovery of clinical candidate **PQR-620** (compound **365**) as a highly potent and selective mTORC1/2 inhibitor, a variety of bridged cyclic rings were investigated to improved selectivity against PI3K. Compound **392**, featuring two morpholines, displayed a high potency, but suffured a low selectivity against PI3K. 8-Oxa-3-azabicyclo[3.2.1]octane ring in compound **393** increased selectivity significantly while keeping a comparable potency. 2-Oxa-5-azabicyclo[2.2.1]heptane ring in compound **394** also increased selectivity significantly while keeping a comparable potency. However, in compound **395** 2-oxa-5-azabicyclo[2.2.1]heptane ring decreased potency dramatically, indicating a preference of chiral conformation. 3-Oxa-6-azabicyclo[3.1.1]heptane ring in compound **396** decreased potency dramatically, although selectivity index was increased to 49 (**Figure 120**). [8]

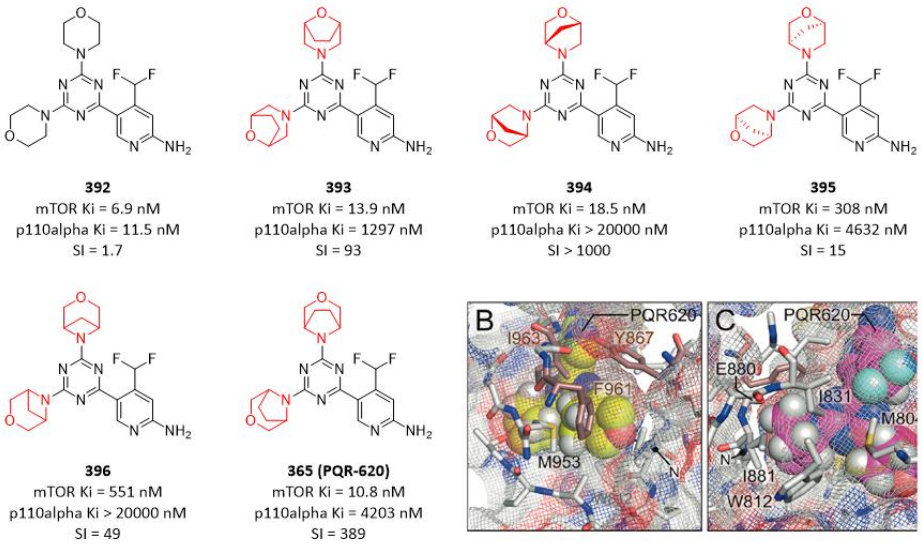

Figure 120. Bridged cyclic rings increased selectivity due to steric clash with protein.

3-Oxa-8-azabicyclo[3.2.1]octane ring in compound **365** (**PQR-620**) increased selectivity significantly with SI = 389, while keeping a comparable potency. Computational modeling studies were used to elucidate the binding mode of compound **365** and ultimately provided structural features defining the compound's high selectivity toward mTOR versus PI3K. The ethylene bridge of the morpholine pointing toward Val882 can take two main conformations, with the bridge oriented toward Met953 defined as bridge-up, or toward Ile881 defined as bridge-down. The bridge-up conformation induces steric clashes within a region of the ATP-binding pocket that has previously been identified as very rigid in PI3K and is defined by residues Tyr867, Phe961 and Ile963. The bridge-down conformation generates steric clash within the backbone of Ile881 and Glu880 and side chains of Ile831 and Ile881. Steric clashes, and as a consequence the weakening of the essential hydrogen bond to the PI3K hinge region explain the reduced affinity of compound **365** for PI3K (**Figure 120**). [8]

As described in above case story, an efficient access of diverse **bridged morpholine building blocks** is of great value for quick exploration of SAR and SPR (**Figure 121**).

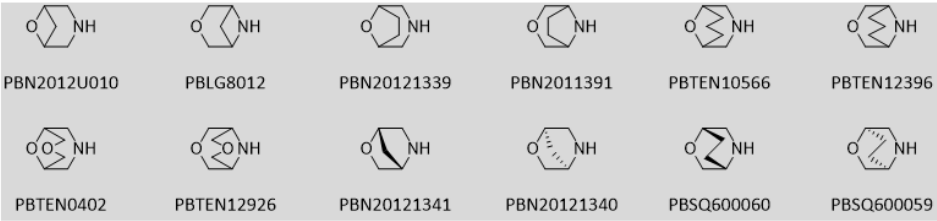

Figure 121. Bridged morpholine building blocks

The trend of selectivity against PI3K in above case story (**Figure 120**) was also observed in another series of mTOR inhibitors. Compared to compound **397** with morpholine ring unsubstituted, 8-oxa-

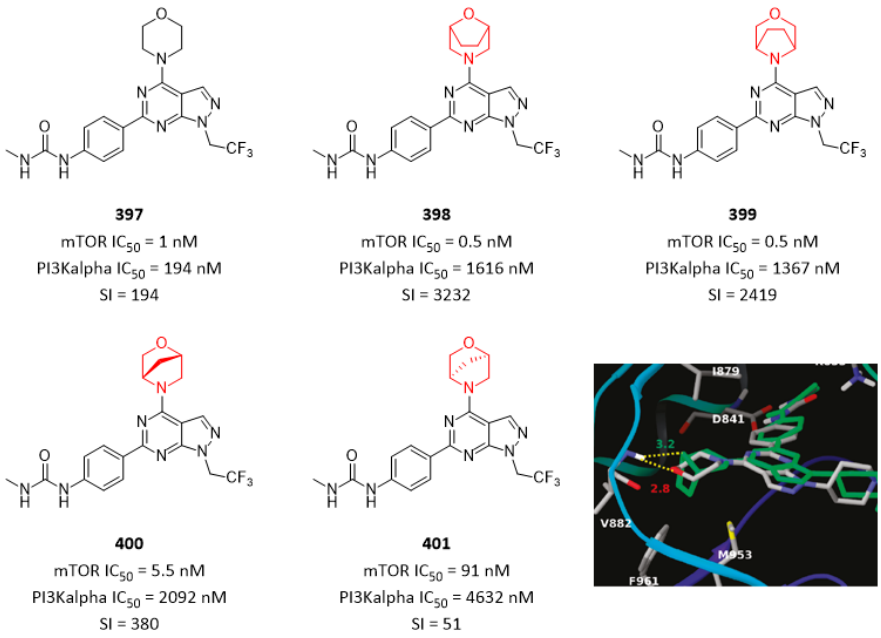

Figure 122. Bridged morpholines increased selectivity due to steric clash.

3-azabicyclo[3.2.1]octane ring in compound **398** and 3-oxa-8-azabicyclo[3.2.1]octane ring in compound **399** both increased selectivity significantly, while keeping comparable potency. However, 2-oxa-5-azabicyclo[2.2.1]heptane rings in compound **400** and compound **401** decreased potency. Docking of the bridged morpholine analogue suggests that a single amino acid difference between mTOR and PI3K causes a difference in the depth of the morpholine binding pockets that is responsible for the increased selectivity observed. Modeling indicates that Phe961 of PI3K is too large to comfortably accommodate the ethylene-bridged morpholine, causing displacement of the morpholine oxygen away from its hydrogen bonding partner, the backbone NH of Val882 (**Figure 122**). [9]

In order to obtain an orally available GSM without covalent binding and phototoxicity, compound **402** was identified as a promising starting point, which has moderate potency and very low human plasma-free fraction and low solubility. By exploring replacements for the central ring with various bridged, bicyclic or azaspiro-piperidine analogues, it was realized that the best replacement was [3.2.1] bridged piperidine as existed in compound **403**. Compound **403** gave an excellent

improvement in potency along with decreased protein binding with human plasma free fraction increased to 40% compared to compound **402**. The potency improvement can be caused by a most favorable conformational change due to the repulsion between the bridge and the lone electron pair from the piperidine nitrogen that enforces an almost linear orientation of the two exit vectors from the piperidine, enabling an optimal binding to gamma-secretase (**Figure 123**). [10]

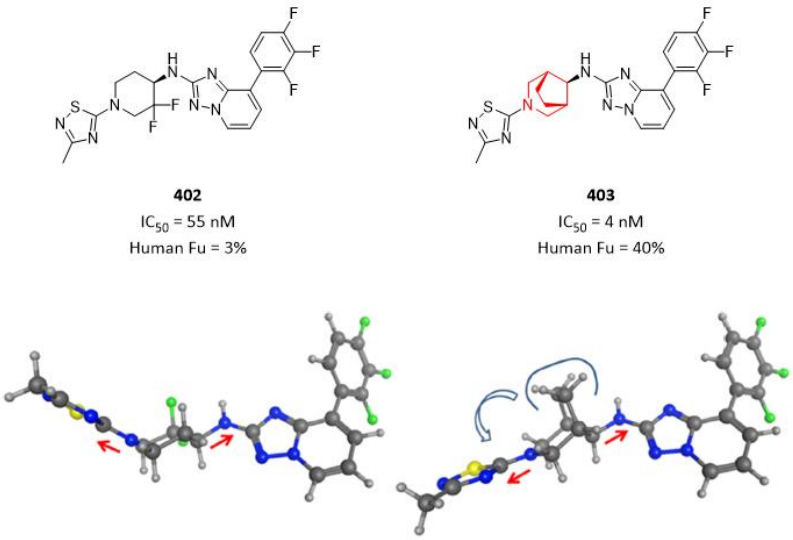

Figure 123. Bridged piperidine increased potency by conformational modulation.

In the course of discovery **EPZ030456** (compound **406**) as the first orally bioavailable small-molecule SMYD3 inhibitor, compound **404** was identified as a promising starting point. Further restriction of conformational freedom with the bridged piperidine core, compound **405**, gave a 17-fold potency improvement over compound **404**. Further optimization led to identification of **EPZ030456** (compound **406**) which displayed stronger potency in cellular assay and demonstrated superior PK profile. To better understand binding model, X-ray crystal structure of compound **406** bound to **SMYD3** was obtained (**Figure 124**). [11]

As described in above two case stories where various bridged piperidine were used to solve critical issues in medicinal chemistry, it is obvious that an efficient access of diverse bridged piperidine building blocks is of great value for medicinal chemists (**Figure 124**).

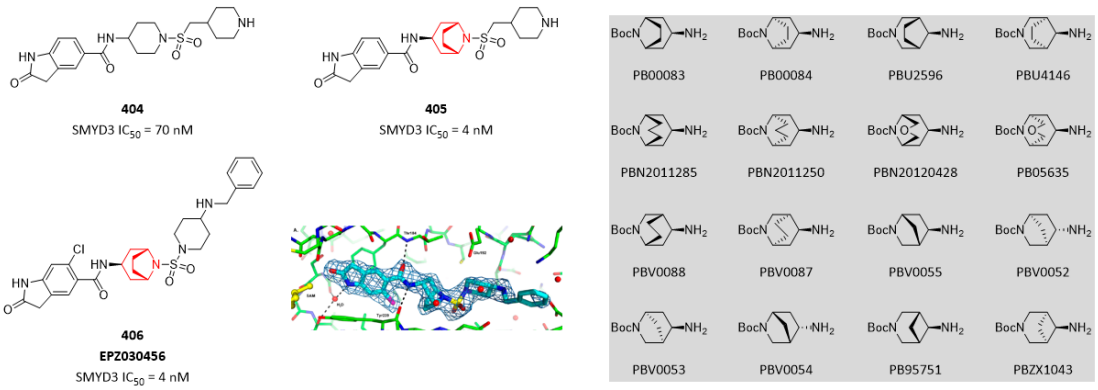

Figure 124. Bridged piperidine increased potency and related building blocks

It was found that compound **408** can fully antagonize an agonist response, while compound **407** can antagonize to approximately 20% of maximum. Taken together with the pharmacology results, the

conformational analysis of compound **407**, compound **408** and compound **409** led the team to propose the agonist conformation hypothesis shown in **Figure 125**. Compound **407** can explore the agonist and antagonist forms from the accessible axial and equatorial conformations and shows partial agonist activity. Compound **408** is constrained to the antagonist conformation and is an antagonist. The agonist conformation is energetically preferred by compound **409**, and this accounts for the greater functional response observed. Complete switching in the functional profile can be attributed to conformational differences in the ligand. [12]

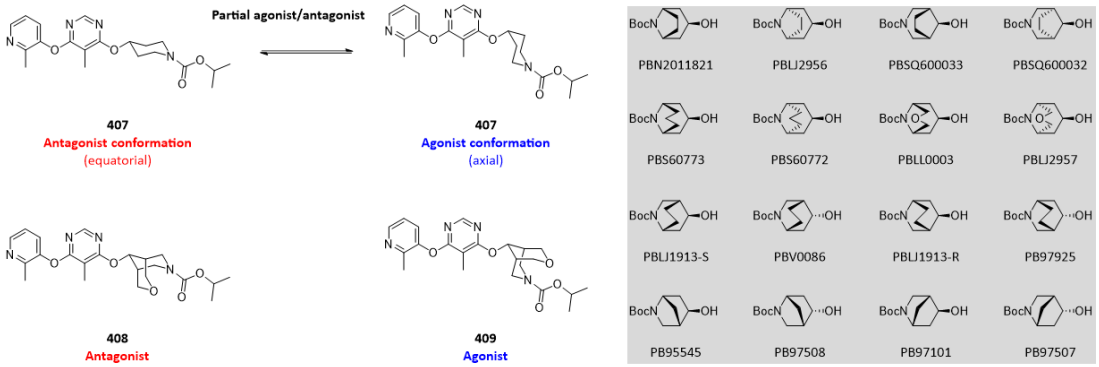

Figure 125. Conformational differences changed mechanism of action.

In order to discover potent, selective, and brain-penetrant LRRK2 inhibitors, the team identified compound **410** as a promising lead compound with high potency. However, this compound suffered very low solubility (< 2 uM), which hinder further development. To address this critical issue, the team focused on disrupting planarity through the introduction of additional complex Fsp^3-riched fragment in the solvent front. With respect to design, the team sought to incorporate fused and/or bridged bicyclic ring systems that, in addition to improving solubility, could also decrease oxidative metabolism of the pyrrolidine and potentially reduce P-gp efflux by further masking the tertiary alcohol polarity. This design logic resulted in the synthesis of azabicyclo[2.1.1]hexane compound **411**, which demonstrated a significantly increased solubility while keeping a comparable potency (**Figure 126**). [13] This kind of caged pyrrolidine building blocks are of great value for exploring SAR and SPR.

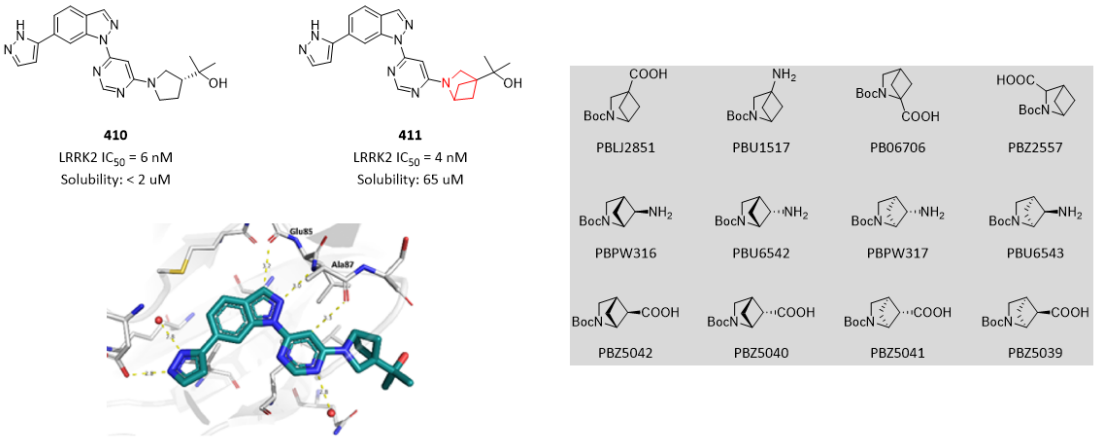

Figure 126. Caged pyrrolidine increased aqueous solubility. (PDB code: 8E80)

Initial evaluation of the SAR from the HTS screen suggested that the diazepane ring found in compound **412** was essential for GCSi activity. Substituted with ethyl group in compound **413**

caused > 10-fold lower potency. However, cyclizing the ethyl group into a 1,4-diazabicyclo[3.2.2]nonane in compound **414** improved the potency > 1000-fold (**Figure 127**). [14]

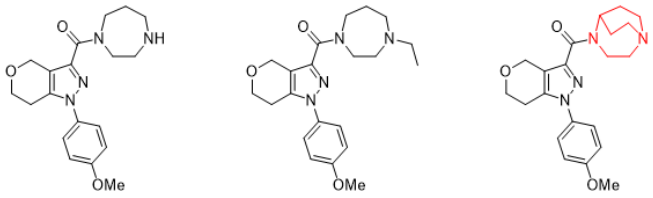

Figure 127. 1,4-Diazabicyclo[3.2.2]nonane increased potency significantly.

References

[1] Sebastien L. Degorce; *et al.* Lowering lipophilicity by adding carbon: one-carbon bridges of morpholines and piperazines. *J. Med. Chem.* **2018**, *61*, 8934-8943.
[2] Andrew Fensome; *et al.* Dual inhibition of TYK2 and JAK1 for the treatment of autoimmune diseases: discovery of ((S)-2,2-difluorocyclopropyl)((1R,5S)-3-(2-((1-methyl-1H-pyrazol-4-yl)amino)pyrimidin-4-yl)-3,8-diazabicyclo[3.2.1]octan-8-yl)methanone (PF-06700841). *J. Med. Chem.* **2018**, *61*, 8597-8612.
[3] Xiaolun Wang; *et al.* Identification of MRTX1133, a noncovalent, potent, and selective KRAS G12D inhibitor. *J. Med. Chem.* **2022**, *65*, 3123-3133.
[4] Changyou Ma; *et al.* Discovery of clinical candidate NTQ1062 as a potent and bioavailable Akt inhibitor for the treatment of human tumors. *J. Med. Chem.* **2022**, *65*, 8144-8168.
[5] Robert G. Gentles; *et al.* Discovery and preclinical characterization of the cyclopropylindolobenzazepine BMS-791325, a potent allosteric inhibitor of the hepatitis C virus NS5B polymerase. *J. Med. Chem.* **2014**, *57*, 1855-1879.
[6] Thomas O. Schrader; *et al.* Discovery of PIPE-359, a brain-penetrant, selective M1 receptor antagonist with robust efficacy in murine MOG-EAE. *ACS Med. Chem. Lett.* **2021**, *12*, 155-161.
[7] Minh H. Nguyen; *et al.* Discovery of orally bioavailable FGFR2/FGFR3 dual inhibitors via structure-guided scaffold repurposing approach. *ACS Med. Chem. Lett.* **2023**, *14*, 312-318.
[8] Denise Rageot; *et al.* Discovery and preclinical characterization of 5-[4,6-bis({3-oxa-8-azabicyclo[3.2.1]octan-8-yl})-1,3,5-triazin-2-yl]-4-(difluoromethyl)pyridine-2-amine (PQR620), a highly potent and selective mTORC1/2 inhibitor for cancer and neurological disorders. *J. Med. Chem.* **2018**, *61*, 10084-10105.
[9] Arie Zask; *et al.* Morpholine derivatives greatly enhance the selectivity of mammalian target of rapamycin (mTOR) inhibitors. *J. Med. Chem.* **2009**, *52*, 7942-7945.
[10] Rosa Maria Rodriguez Sarmiento; *et al.* Stepwise design of r-secretase modulators with an advanced profile by judicious coordinated structural replacements and an unconventional phenyl ring bioisostere. *J. Med. Chem.* **2020**, *63*, 8534-8553.
[11] Lorna H. Mitchell; *et al.* Novel oxindole sulfonamides and sulfamides: EPZ031686, the first orally bioavailable small molecule SMYD3 inhibitor. *ACS Med. Chem. Lett.* **2016**, *7*, 134-138.
[12] Kim F. McClure; *et al.* Activation of the G-protein-coupled receptor 119: a conformation-based hypothesis understanding agonist response. *J. Med. Chem.* **2011**, *54*, 1948-1952.
[13] David A. Candito; *et al.* Discovery and optimization of potent, selective, and brain-penetrant 1-heteroaryl-1H-indazole LRRK2 kinase inhibitors for the treatment of Parkinson's disease. *J. Med. Chem.* **2022**, *65*, 16801-16817.

[14] Anthony J. Roecker; *et al.* Pyrazole ureas as low dose, CNS penetrant glucosylceramide synthase inhibitors for the treatment of Parkinson's disease. *ACS Med. Chem. Lett.* **2023**, *14*, 146-155.

Cyclopropane in Medicinal Chemistry

Cyclopropyl ring has been playing versatile roles in drug discovery, as can be seen from approved drug and clinical candidate molecules (**Figure 128**). Important features of the cyclopropyl ring are: 1) coplanarity of the three carbon atoms, 2) relatively shorter C-C bonds, 3) enhanced pi-character of C-C bonds, and 4) C-H bonds are shorter and stronger than those in alkanes. These distinct features confer cyclopropyl ring with great value in molecule design and ability to address multiple critical issues that can occur during drug discovery such as: a) enhancing potency, b) increasing selectivity, c) increasing metabolic stability, d) increasing permeability and BBB-penetration, e) increasing solubility, f) contributing to an entropically more favorable binding to target and g) improve PK profile. Cyclopropyl ring can be exploited either as a substituent, as a chiral bridge, and as a spiro or fused ring (discussed in previous sections) in solving multiple challenges that occurs during the course of drug discovery program. [1]

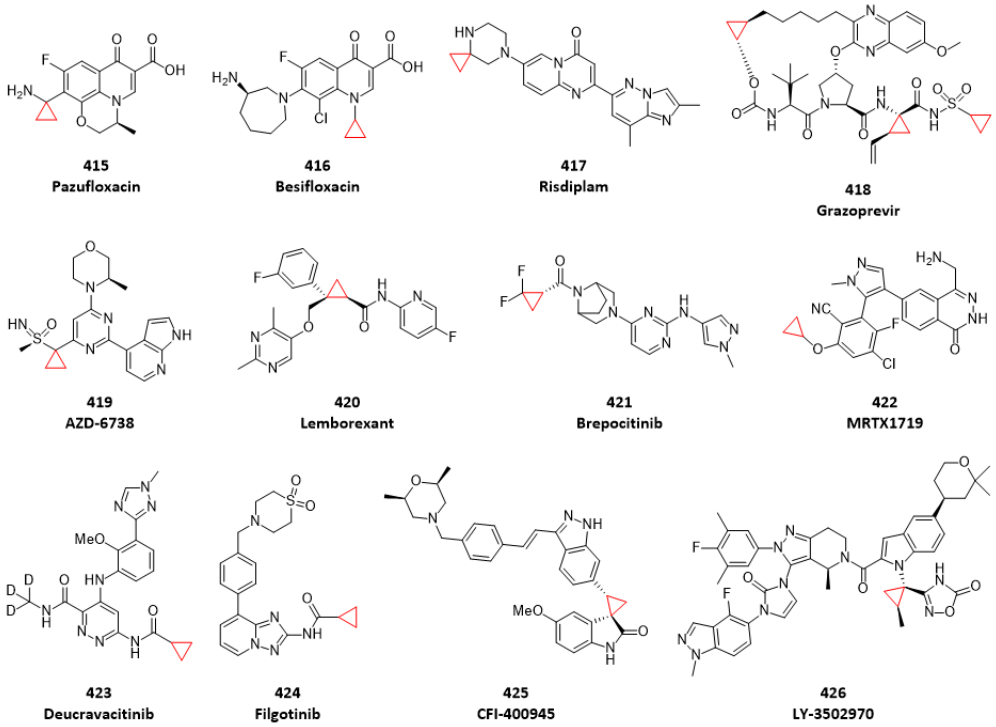

Figure 128. Approved drug and clinical candidate molecules containing cyclopropyl rings

Cyclopropanes and other hydrocarbons containing three-membered rings have a certain sp2 character and gain substantial H-bond acidity which can serve as a hydrogen bond donor. In the course of discovery of **Filgotinib** (compound **424**) as a selective JAK1 inhibitor, compound **429** was identified as a primary hit with modest JAK1 inhibition. Replacement of the cyclopropyl amide moiety showed the importance of this position on the activity. Surprisingly, close amide analogues, such as isopropylamide **428** or acetamide **427** displayed much reduced potency against JAK1. Addition of a methyl group on cyclopropane in compound **429** was also detrimental to JAK1 inhibition. Only the crystal structure of **Filgotinib** (compound **424**) obtained later gave a possible explanation for this SAR observations. It was hypothesized that the superior ability of the cyclopropane ring to donate an H-bond could explain the SAR observations. The crystal structure demonstrates a putative hydrogen bond between the C-H of the cyclopropylamide and the carbonyl

oxygen of Leu932 and of Pro933 (**Figure 129**). This type of interaction has been previously described in the literature. [2-3]

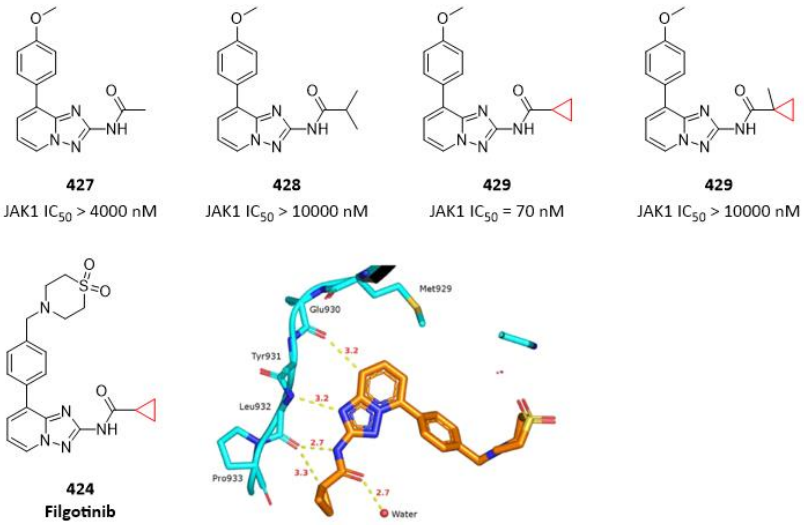

Figure 129. C-H of cyclopropylamide serves as a hydrogen bond donor. (PDB code: 4P7E)

The special ability to serve as a hydrogen bond donor makes cyclopropane-1-carboxylic acid building blocks of great value for molecule design (**Figure 130**).

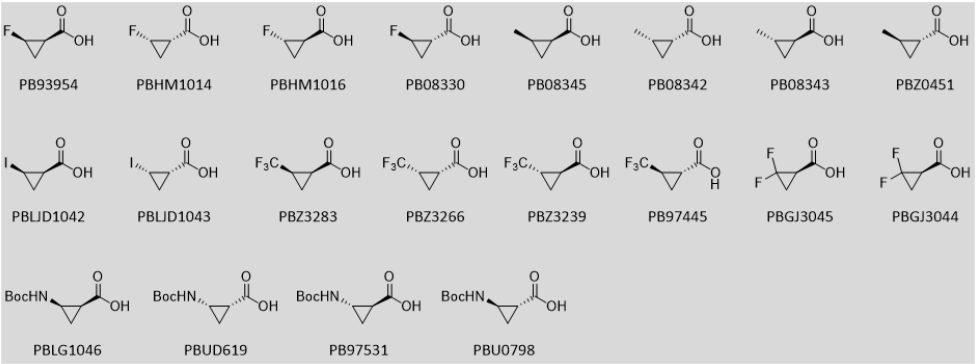

Figure 130. Cyclopropane-1-carboxylic acid building blocks

In the course of discovery of **MRTX1719** (compound **422**) as a synthetic lethal inhibitor of the PRMT5 MTA complex for the treatment of MTAP-deleted cancers, compound **430** was identified from a fragment-based campaign which displayed a modest cellular potency. In order to further increase cellular potency, X-ray crystal structure indicated that there was a small lipophilic pocket sandwiched between Phe300 and Tyr304 around methoxyl group of compound **430**. With this in mind, a variety of small, lipophilic substituents on oxygen were examined. Among of them, cyclopropane ring in compound **431** demonstrated increased cellular potency by 7-fold. Further optimization based on compound **431** aiming to increase cellular potency and improve ADMET profile led to identification of **MRTX1719** (compound **422**). The X-ray crystal structure of **MRTX1719** (compound **422**) bound to PRMT5 MTA demonstrated that cyclopropane ring occupied the small lipophilic pocket sandwiched between Phe300 and Tyr304 (**Figure 131**). [4]

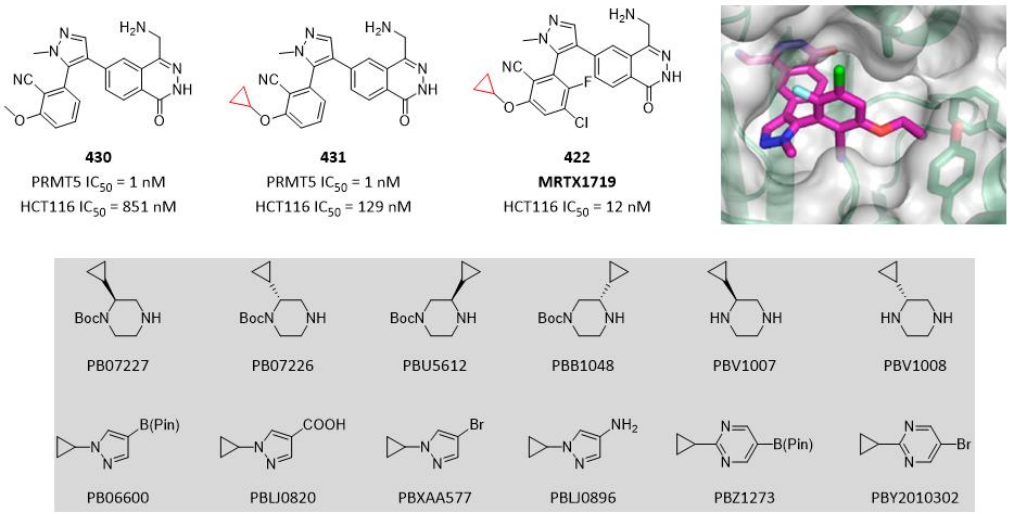

Figure 131. Cyclopropane ring increased potency by occupying a small lipophilic pocket. (PDB code: 7S1S)

Compound **432** was discovery by a fragment-based drug discovery (FBDD) campaign, which was a potent PDE10 inhibitor. The team sought to functionalize selected positions in the aliphatic chain with the goal of blocking possible sites of metabolism. It was soon realized that significant improvements by incorporation of cyclopropane constraint in compound **433** and compound **434**. While the potency of *cis*-cyclopropane linker in compound **433** was compromised relative to compounds with more flexible linkers, the corresponding *trans*-cyclopropane linker in compound **434** provided a dramatic improvement in potency (> 10-fold). Further optimization of compound **434** led to discovery of compound **435** with more promising ADMET and PK profiles which was advanced to *in vivo* study (**Figure 132**). [5]

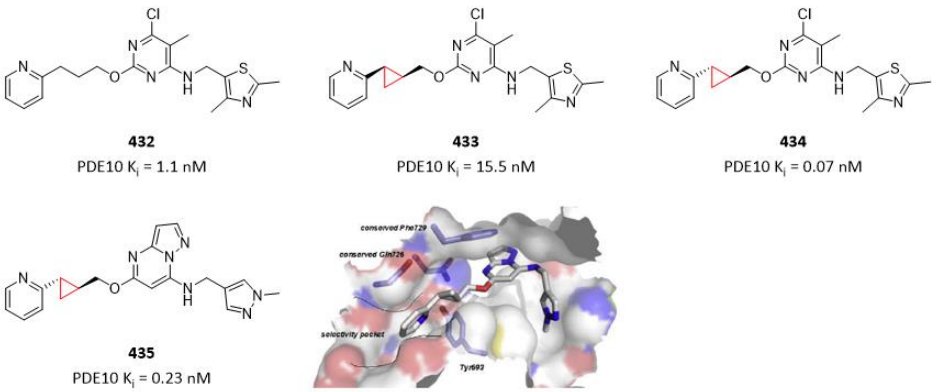

Figure 132. Cyclopropane linker increased potency by locking conformation. (PDE code: 5DH5)

In the course of discovery of clinical candidate **CFI-400945** (compound **425**) as a PLK4 selective inhibitor, compound **436** was identified as a promising hit. In order to lock the molecule into a stable configuration, it was computationally to predict whether compound activity would be retained upon replacing the *E*-alkene in compound **436** with the *trans*-cyclopropane in compound **437**. PLK4 docking predicted retention of activity for this bioisostere replacement. It can be seen that the *E*-form of compound **436** and *1R,2S* stereoisomer **437** have nearly identical topology and similar binding poses. It was equally pleasing to see that compound **437** was active against PLK4 and performed favorably with respect to compound **436** in terms of selectivity toward FLT3 and KDR. Furthermore, it was found that the cyclopropane modification imparts improved aqueous solubility. This improvement is attributed to the nature of the cyclopropane ring, being orthogonal to the

plane of the indolinone, it serves to counter crystal packing forces. Compound **437** also demonstrated desirable ADMET properties, which included an improved profile for CYP isomers, and better microsome stability. More significantly, compound **437** achieved up to 100-fold higher level of exposure in mouse plasma. Further optimization led to discovery of compound **438** and clinical candidate **CFI-400945** (compound **425**) (**Figure 133**). [6]

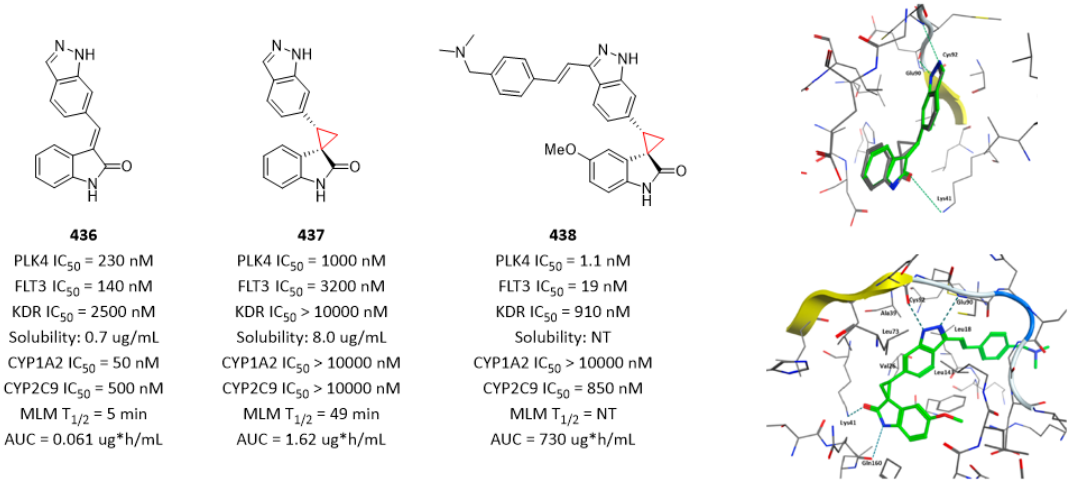

Figure 133. Cyclopropane addressed selectivity and ADMET profile issues. (PDB code: 4JXF)

From above two case stories, 2-phenylcyclopropane building blocks are of great value as bioisosteres of styrene, potentially addressing critical issues associated with styrene (**Figure 134**).

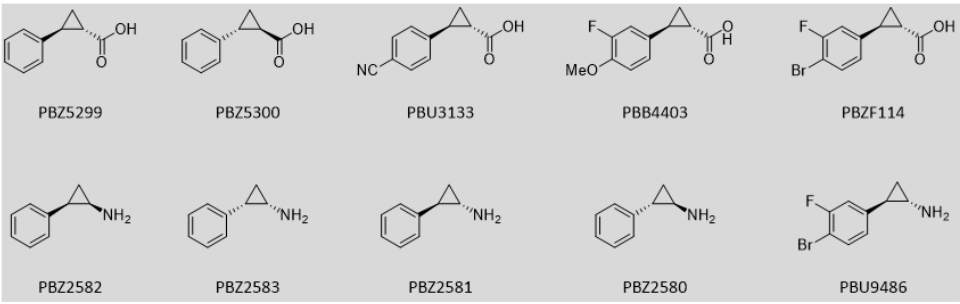

Figure 134. 2-Phenylcyclopropane building blocks as bioisosteres of styrene

Guided by the model, the prime side SAR was further explored by introducing structural features designed to more effectively complement the uniquely defined S1' subsite. Most immediately, the cyclopropylacylsulfonamide compound **441** was evaluated and this compound inhibited HCV NS3/4A activity with IC_{50} of 1 nM, which is 30-fold potent than compound **439**. Close analogues were significantly less active, with ethylacylsulfonamide compound **440** showing 6-fold reduced activity, isopropylacylsulfonamide compound **442** showing 19-fold reduced activity, and cyclobutylacylsulfonamide compound **443** showing 7-fold reduced activity. It can be concluded that this specific aliphatic binding element was critical to activity while also sensitive to small structural modification. These prime side SAR were rationalized using a plot of the van der Waals surface of the protein which highlights the shallow cavity within the S1' site that is defined by Gln41, Phe43, Val55 and Gly58. An assessment of the optimized geometries of the sulfonamide caps suggested that the cyclopropane exhibited a shape most complementary with the S1' pocket, thus maximizing van der Waals surface contact and explaining the potency of compound **441** (**Figure 135**). [7]

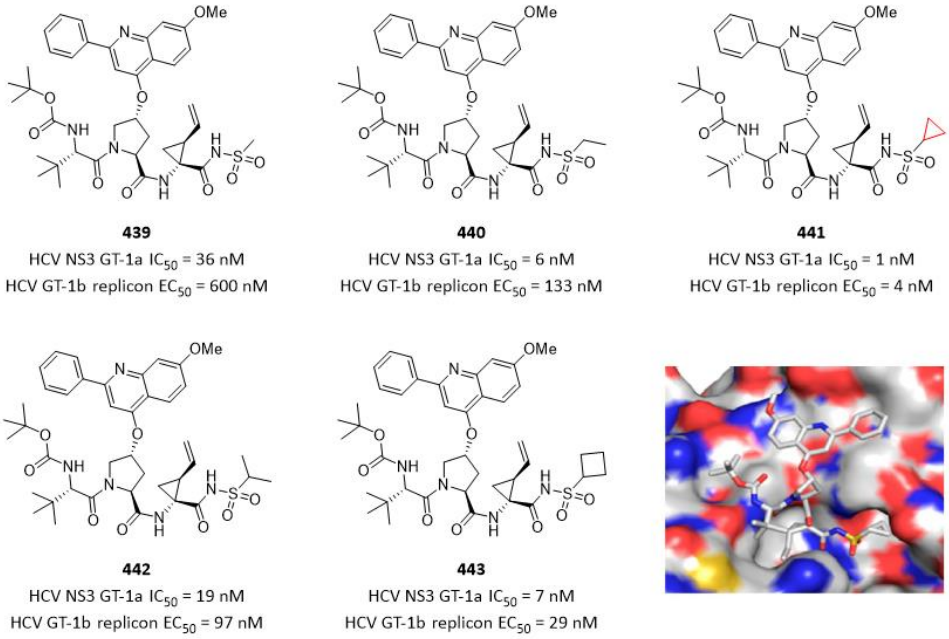

Figure 135. Cyclopropane increased anti-HCV potency by occupying a small hydrophobic pocket.

In the lead optimization course of small-molecule IL-17 inhibitors, although compound **444** gave the best potency, it came with significant metabolic instability in human live microsome. In contrast, biscyclopropylalanine compound **445** was stable in human liver microsome even with the increased lipophilicity. The X-ray crystal structure of compound **445** bound to IL-17 revealed that the biscyclopropyl moiety makes hydrophobic contacts with Tyr85, Leu120, Leu122, and Leu135 of subunit B (**Figure 136**). [8]

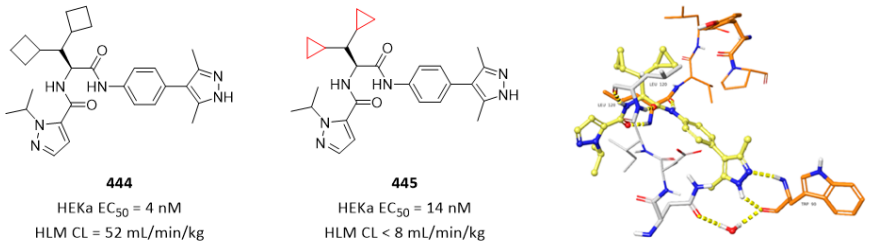

Figure 136. Cyclopropane increased metabolic stability in human liver microsome. (PDB code: 7AMA)

Further development of compound **446** was hampered by realization that this scaffold formed reactive metabolites. To overcome this metabolic liability, the team discovered that the problematic diaminopyridine scaffold could be efficiently replaced with a cyclopropylamino acid moiety. The design concept yielded compound **447** with an improved PK profile (**Figure 137**). [9]

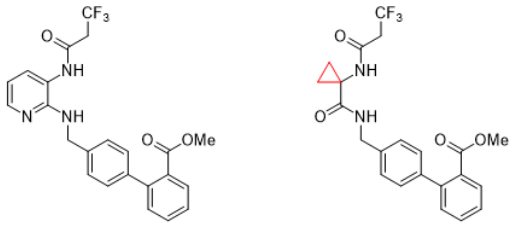

446
hBK1 K_i = 12 nM
$T_{1/2}$ = 0.2 h
CL = 35 mL/min/kg
F: 9%

447
hBK1 K_i = 63 nM
$T_{1/2}$ = 9.5 h
CL = 9.3 mL/min/kg
F: 26%

Figure 137. Cyclopropylamino acid amide as a bioisostere of 2,3-diaminopyridine

References

[1] Tanaji T. Talele. The “cyclopropyl fragment” is a versatile player that frequently appears in preclinical/clinical drug molecules. *J. Med. Chem.* **2016**, *59*, 8712-8756.
[2] Ibon Alkorta; *et al.* Ring strain and hydrogen bond acidity. *J. Org. Chem.* **1998**, *63*, 7759-7763.
[3] Christel J. Menet; *et al.* Triazolopyridines as selective JAK1 inhibitors: from hit identification to GLP0634. *J. Med. Chem.* **2014**, *57*, 9323-9342.
[4] Christopher R. Smith; *et al.* Fragment-based discovery of MRTX1719, a synthetic lethal inhibitor of the PRMT5 MTA complex for the treatment of MTAP-deleted cancers. *J. Med. Chem.* **2022**, *65*, 1749-1766.
[5] Izzat T. Raheem; *et al.* Discovery of pyrazolopyrimidine phosphodiesterase 10A inhibitors for the treatment of schizophrenia. *Bioorg. Med. Chem. Lett.* **2016**, *26*, 126-132.
[6] Peter B. Sampson; *et al.* The discovery of Polo-like kinase 4 inhibitors: design and optimization of spiro[cyclopropane-1,3’[3H]indol]-2’(1’H)-ones as orally bioavailable antitumor agents. *J. Med. Chem.* **2015**, *58*, 130-146.
[7] Paul M. Scola; *et al.* Discovery and early clinical evaluation of BMS-605339, a potent and orally efficacious tripeptidic acylsulfonamide NS3 protease inhibitor for the treatment of hepatitis C virus infection. *J. Med. Chem.* **2014**, *57*, 1708-1729.
[8] Mark D. Andrews; *et al.* Discovery of an oral, rule of 5 compliant, interleukin 17A protein-protein interaction modulator for the potential treatment of psoriasis and other inflammatory diseases. *J. Med. Chem.* **2022**, *65*, 8828-8842.
[9] Michael R. Wood; *et al.* Cyclopropylamino acid amide as a pharmacophoric replacement for 2,3-diaminopyridine. Application to the design of novel bradykinin B1 receptor antagonists. *J. Med. Chem.* **2006**, *49*, 1231-1234.

Nitrile in Medicinal Chemistry

The nitrile group has played an increasingly important role in medicinal chemistry, with more than 60 small-molecule approved drugs and a tremendous number of clinical candidates containing nitrile (**Figure 138**). [1-3] Since 2010, the FDA has approved at least one nitrile-containing drug every year, and reached the maximum number of five drugs in 2020. The marketed drugs with a nitrile moiety target a wide range of clinical disorders, including heart failure, hypertension, chronic myeloid leukemia, breast cancer, virus infection, etc.

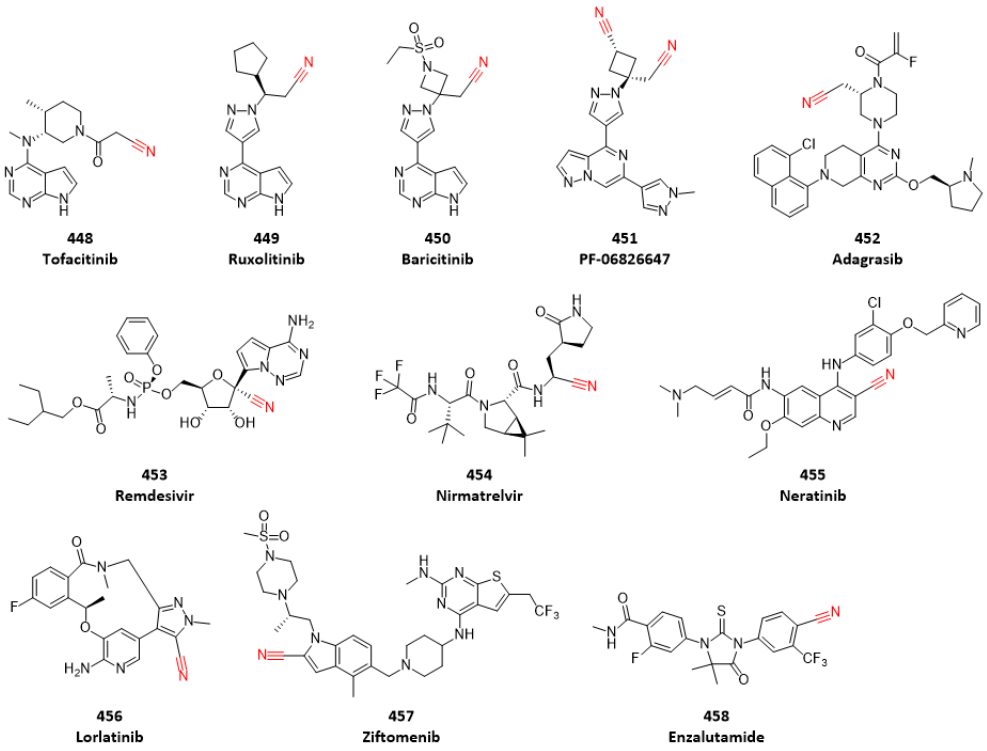

Figure 138. Approved drugs and clinical candidates containing nitrile group

Underpinning a wide range of applications of nitrile group in drug discovery are its unique features, including but not limited to the followings (**Figure 139**): [1-3]

a) Owing to its linear shape and low molecular volume, nitrile group can properly fit in the subsites of proteins and perform lipophilic interactions *via* the triple bond π system. The molecular volume of nitrile group is only one-eighth the size of methyl group, with 1.16 Å length of CN triple bond.

b) The carbon atom can act as an electrophile due to its electron deficiency, promoted by the high electronegativity of the nitrogen atom and high dipole moment in the triple bond; while the nitrogen atom can act as a hydrogen bond acceptor by its lone pair. So a nitrile group can simultaneously form two interactions with protein.

c) In addition to the non-bonded interactions, nitrile is a remarkable group that can for covalent adduct with proteins, mainly linked to a reactive cysteine or serine side chain. The most popular examples are DDP-4 inhibitors (**Vildagliptin** and **Saxagliptin**) and 3CL inhibitors (**Nirmatrelvir**).

d) Compounds containing nitrile group generally have a lower cLogP which indicates enhanced solubility. Compared to alkyne, nitrile decreases cLogP by 0.84 unit.

e) Nitrile group is considerably metabolically stable and non-toxic. It usually remains unchanged when it is eliminated from human body.

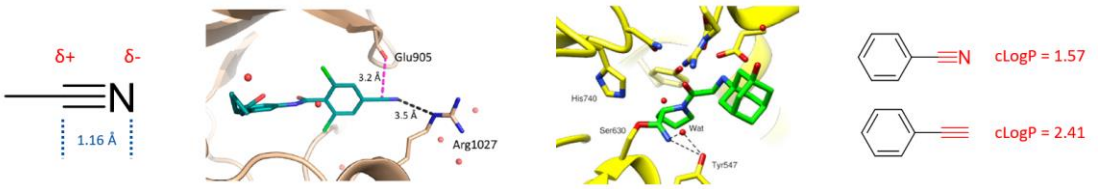

Figure 139. Unique features of nitrile group: an example where nitrile forms two interactions with protein (PDB code: 4GI1); [11] an example where nitrile forms a covalent bond with protein (PDB code: 6B1E); [2] compared to alkyne, nitrile decreases cLogP by 0.84 unit.

In the course of discovery of clinical candidate **Adagrasib** (compound **452**), in order to increase potency of compound **459**, X-ray crystal structure was obtained. Notable in this crystal structure is a bound water molecule complexed to Gly10 and Thr58 which is near the piperazine ring. This water molecule forms hydrogen bonds with the side chain hydroxyl of Thr58 and the carbonyl of Gly10. Analysis of the proximal hydrogen bonding network suggested that displacement of this water could lead to a large potency increase. An appropriately substituted piperazine ring would have the correct trajectory to displace this bound water. With this hypothesis in mind, a series of analogues were designed and synthesized. Among of them, compound **460** with *S*-CH_2CN was determined to be 440-fold more potent than compound **459** and 100-fold more potent than diastereomer **461**. In addition to binding, CH_2CN also impacted chemical reactivity of acrylamide. For example, compound **459** has a GSH $T_{1/2}$ = 17 h; on the hand, compound **460** and compound **461** have significantly decreased GSH $T_{1/2}$ = 4 h and 1 h respectively. Further optimization based on compound **460** led to identification of **Adagrasib** (compound **452**). X-ray crystal structure of **Adagrasib** (compound **452**) bound to KRAS G12C revealed that nitrile displaces the Gly10 bound water and forms a hydrogen bond to the backbone NH of Gly10 (**Figure 140**). [4]

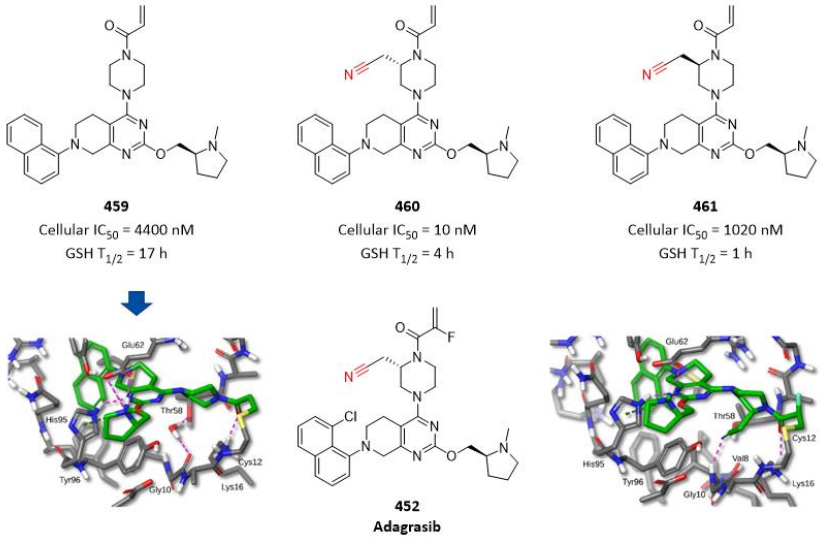

Figure 140. Nitrile displaces water molecule and increased potency. (PDB codes: 6USX, 6UT0)

In the course of discovery of clinical candidate **PF-06826647** (compound **451**) as a selective TYK2 inhibitor, compound **462** was identified as a promising lead compound. X-ray crystal structure of compound **462** bound to TYK2 revealed that the positioning of the alkyl cyano group was shown to be toward the C-terminal lobe in the active site lower lipophilic pocket. The trifluoromethyl azetidine group provided the desired TYK2 potency through engagement of the P-loop, but the overall moderate LipE reflected the high overall lipophilicity of the molecule. In order to improve the modest metabolic stability as judged by human liver microsome turnover, the team attempted to replace trifluoroethylamino group. In addition, replacement of the trifluoroethylamino group

was preferred due to association with testicular toxicity liability for potential metabolites. Unique within this series, the cyanomethyl group of compound **463** recapitulated the potency of compound **462**, and also lowered HLM clearance. Further optimization based on compound **463** led to identification of **PF-06826647** (compound **451**). X-ray crystal structure of **PF-06826647** (compound **451**) bound to TYK2 revealed that the *cis*-cyclobutanecarbonitrile moiety was positioned below and toward the tip of the P-loop. The end of the P-loop contains mainly hydrophobic residues and a generally satisfied hydrogen bond network which may contribute to the calculated lability of this modeled water in the apo structure. This predicted high energy water is displaced by the cyclobutanecarbonitrile group of **PF-06826647** (compound **451**). The electrostatic mapping of this pocket also showed a positive electrostatic potential which could provide a favorable interaction with the cyano group (**Figure 141**). [5]

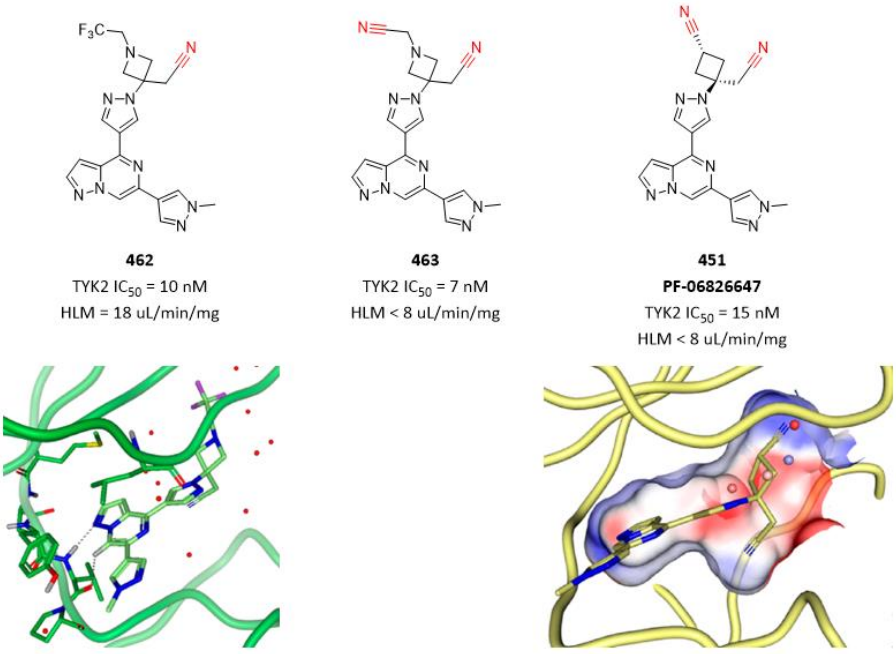

Figure 141. Nitrile replace water molecule and increased metabolic stability. (PDB codes: 6X8F, 6X8G)

Nirmatrelvir inhibits the SARS-CoV-2 main protease, also known as 3C-like protease ($3CL^{pro}$), which plays a crucial role in cleaving the coronavirus polyprotein to form smaller essential proteins required for virus replication and pathogenesis. Nitrile in **Nirmatrelvir** forms a covalent bond with Cys145 of $3CL^{pro}$, which is a critical interaction for high potency. Removing nitrile in compound **464** lost potency completely, while transforming nitrile to amide in compound **465** also lost potency completely, suggesting that an electrophilic warhead is essential for inhibiting 3CL (**Figure 142**). [6] X-ray crystal structure of **Nirmatrelvir** bound to $3CL^{pro}$ revealed that there is a covalent bond between nitrile and Cys145.

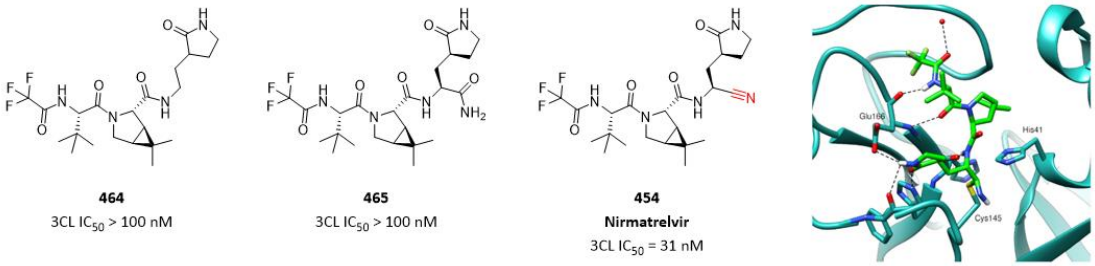

Figure 142. Nitrile forms a covalent bond with Cys145. (PDB code: 7RFW)

Vildagliptin (compound **466**) and **Saxagliptin** (compound **467**), which are DDP-4 inhibitors, can form a reversible covalent bond with Ser630. Their binding modes were characterized by the crystal structure of these inhibitors bound to the enzyme in the covalent state (**Figure 143**). [2]

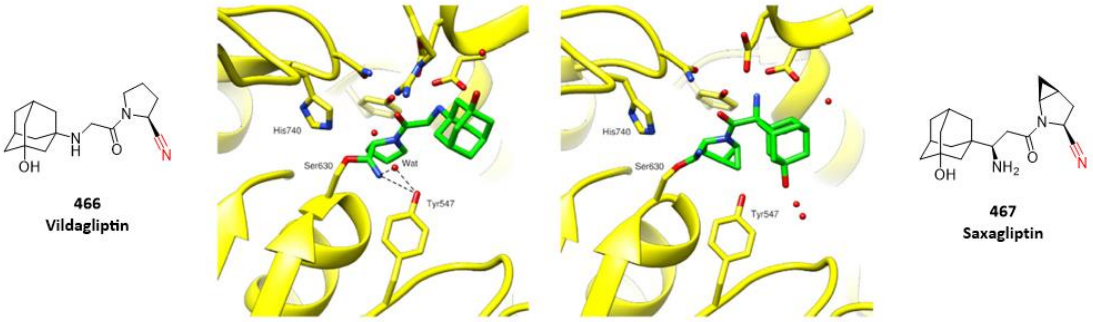

Figure 143. Nitrile in DDP-4 inhibitors can form covalent bond with Ser630. (PDB codes: 6B1E, 3BJM)

As described in above examples, aliphatic building blocks containing nitrile are of great value for discovery of covalent inhibitors (**Figure 144**).

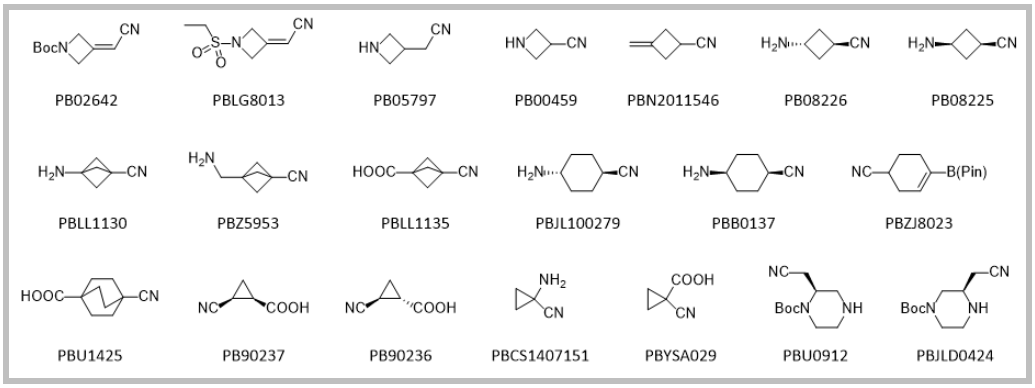

Figure 144. Aliphatic building blocks containing nitrile

It was found that 4-anilinoquinoline-3-carbonitrile **468** is an effective inhibitor of EGFR with activity comparable to 4-anilinoquinazoline **469**. A new homology model of EGFR was constructed based on the X-ray structures of Hck and FGF receptor-1 kinase. The model suggests that with the quinazoline-based inhibitor, the N3 atom is hydrogen bonded to a water molecule which, in turn, interacts with Thr830. It is proposed that the quinolone-3-carbonitrile bind in a similar manner where the water molecule is displaced by the cyano group which interacts with the same Thr830 residue (**Figure 145**). [7]

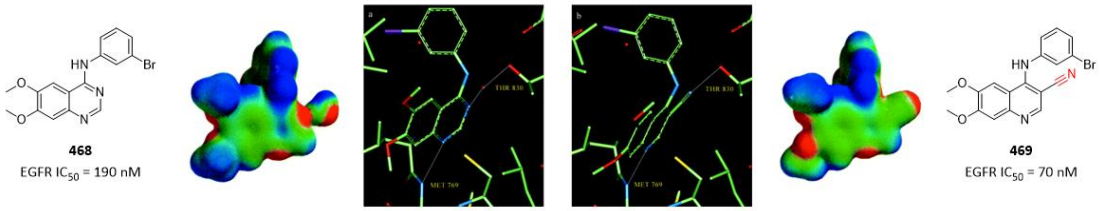

Figure 145. Nitrile displace water molecule, and forms hydrogen bond directly with Thr830.

Based on above findings, several EGFR inhibitors were discovered and approved. One of them is **Neratinib**, a covalent EGFR inhibitor with nitrile forming a hydrogen bond with protein directly (**Figure 146**). [8]

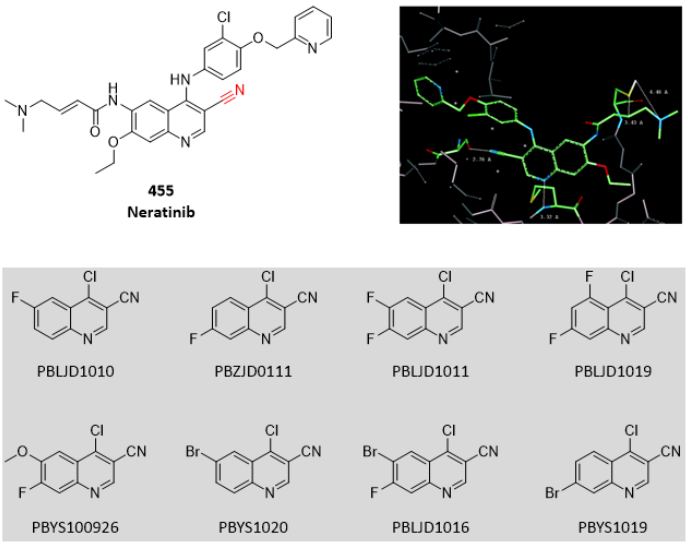

Figure 146. Nitrile in **Neratinib** forms a hydrogen bond with protein directly.

Replication of SARS-CoV-2 depends on the viral RNA-dependent RNA polymerase (RdRp), which is the target of the **Remdesivir** (compound **453**), a pro-drug of compound **473**. **Remdesivir** shows broad-spectrum antiviral activity against RNA viruses, and previous studies with RdRps from Ebola virus and Middle East respiratory syndrome coronavirus (MERS-CoV) have revealed that delayed chain termination is **Remdesivir**'s mechanism of action. [9] Comparing compound **470**, compound **471**, compound **472** and compound **473**, these data established that 1'-CN group was optimal among several 1'-modifications on the adenine C-nucleoside for RSV potency. [10] Structural studies demonstrated that 1'-CN of **Remdesivir** sits in a pocket formed by residues Thr-687 and Ala-688 at the beginning of chain prolongation. At i+4, 1'-CN moiety encounters a steric clash with Ser-861, and prevents RdRp from advancing into i+4, resulting in chain termination (**Figure 147**).

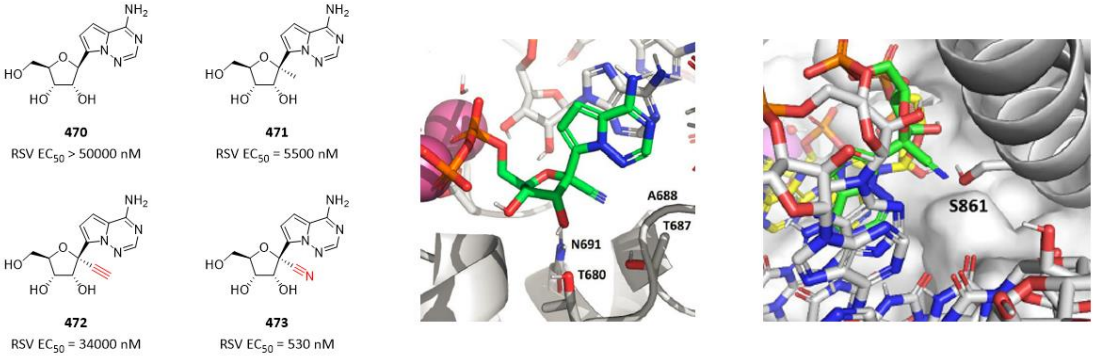

Figure 147. Critical role of 1'-CN and mechanism of action of Remdesivir

Based on compound **474**, addition of a Br in compound **475** increased biochemical potency, but did not increased cellular potency proportionally. It was surprisingly that addition of a cyano in compound **476** increased both biochemical potency and cellular potency significantly. Docking model revealed that the nitrogen atom of nitrile of compound **476** forms a hydrogen bond with Lys590 of protein (**Figure 148**). [12]

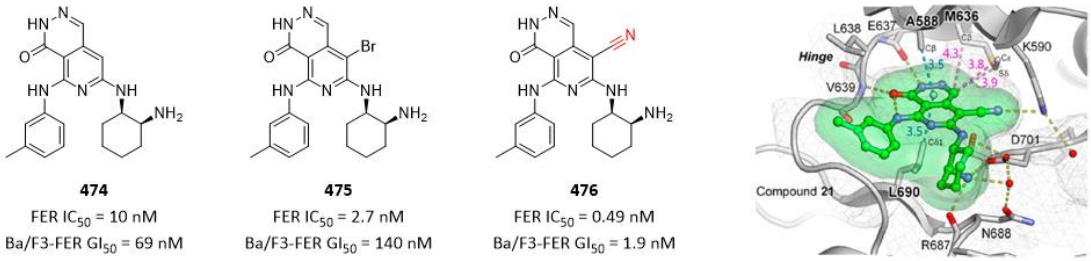

Figure 148. Nitrile increased potency by forming a hydrogen bond with protein.

In the course of discovery **Lorlatinib** (compound **456**) as a selective ALK inhibitor, to increase selectivity of compound **477** against TrkB and other kinases, the team employed the residue difference between ALK (Leu1198) and TrkB (Tyr635). The pyrazole cyano moiety in **Lorlatinib** (compound **456**) was efficient for obtaining selectivity because the cyano contains only one more heavy atom than the unselective methyl analogue **477** and gains at least 35-fold selectivity. It is hypothesized that the nitrile makes an unfavorable contact with the CE atom of the Tyr635 in TrkB, closer to the midpoint of the side chain rather than at the terminus. Unfavorable desolvation penalties or electrostatics due to the proximity of the electron-rich nitrile nitrogen atom and tyrosine may further enhance selectivity (**Figure 149**). [13]

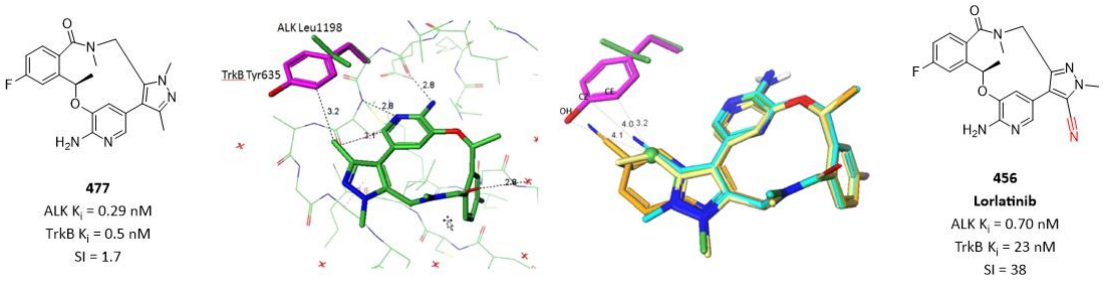

Figure 149. Nitrile increased selectivity. (PBD codes: 4CMU, 4AT3, 4CLI)

A HSQC-based screening of 13,000 fragments revealed 20 fragments hits that displayed chemical shift perturbation patterns of KRAS G12V different than those observed with compounds that bind to switch I/II. Among these compounds was a cluster that included both aminocyanothiophenes and aminothiazoles. NMR titration of the hits using the modified KRAS construct revealed that fragment hit **478** bound to the modified protein with an affinity of 116 uM. Aminothiazole fragment hit **479** showed reduced affinity compared to fragment hit **478**. Using a combination of targeted commercial purchasing and discrete compound synthesis, the cyano group is shown to be important based on complete loss of affinity observed for compound **480**. X-ray crystal structure of fragment hit **478** bound to GDP-KRAS G12V revealed that nitrile interacts with both the amide NH of Glu63 as well as nearby bound water. This network of interactions readily explains the rigid requirement for nitrile for the best affinity (**Figure 150**). [14]

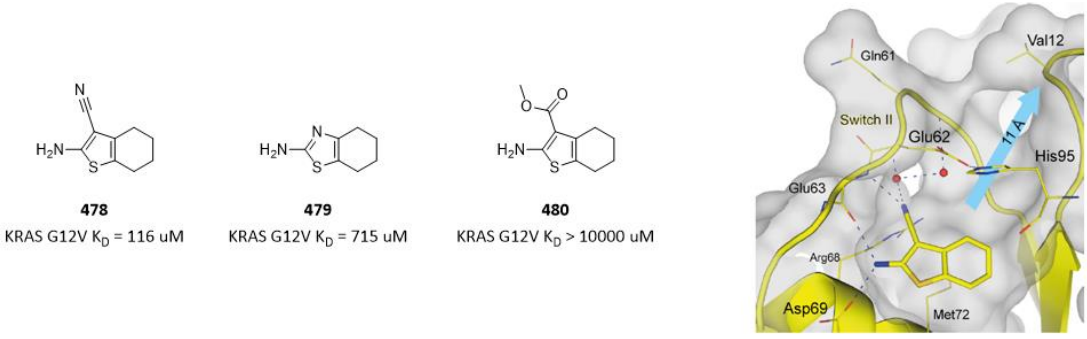

Figure 150. Nitrile interacts with both NH of backbone and nearby bound water. (PDB code: 7U8H)

The above described cases displayed great value of aromatic nitrile building blocks for quick exploration of SAR and SRP (**Figure 151**).

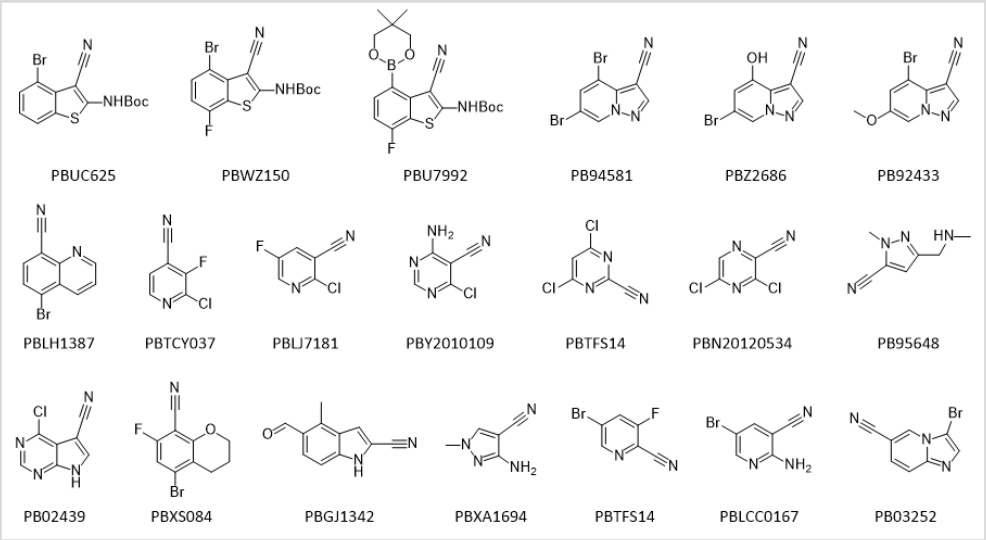

Figure 151. Aromatic nitrile building blocks

References

[1] Xi Wang; *et al.* Nitrile-containing pharmaceuticals: target, mechanism of action, and their SAR studies. *RSC Med. Chem.* **2021**, *12*, 1650-1671.
[2] Vinicius Bonatto; *et al.* Nitriles: an attractive approach to the development of covalent inhibitors. *RSC Med. Chem.* **2023**, *14*, 201-217.
[3] Fraser F. Fleming; *et al.* Nitrile-containing pharmaceuticals: efficacious roles of the nitrile pharmacophore. *J. Med. Chem.* **2010**, *53*, 7902-7917.
[4] Jay B. Fell; *et al.* Identification of the clinical development candidate MRTX849, a covalent KRAS G12C inhibitor for the treatment of cancer. *J. Med. Chem.* **2020**, *63*, 6679-6693.
[5] Brian S. Gerstenberger; *et al.* Discovery of tyrosine kinase 2 (TYK2) inhibitor (PF-06826647) for the treatment of autoimmune diseases. *J. Med. Chem.* **2020**, *63*, 13561-13577.
[6] Subramanyam Vankadara; *et al.* A warhead substitution study on the Coronavirus Main Protease inhibitor Nirmatrelvir. *ACS Med. Chem. Lett.* **2022**, *13*, 1345-1350.
[7] Allan Wissner; *et al.* 4-Anilino-6,7-dialkoxyquinoline-3-carbonitrile inhibitors of epidermal growth factor receptor kinase and their bioisosteric relationship to the 4-anilino-6,7-dialkoxyquinazoline inhibitors. *J. Med. Chem.* **2000**, *43*, 3244-3256.
[8] Hwei-Ru Tsou; *et al.* Optimization of 6,7-disubstituted-4-(arylamino)quinolone-3-carbonitriles as orally active, irreversible inhibitors of human epidermal growth factor receptor-2 kinase activity. *J. Med. Chem.* **2005**, *48*, 1107-1131.
[9] Calvin J. Gordon; *et al.* Remdesivir is a direct-acting antiviral that inhibits RNA-dependent RNA polymerase from severe acute respiratory syndrome coronavirus 2 with high potency. *J. Biol. Chem.* **2020**, *295*, 6785-6797.
[10] Richard L. Mackman; *et al.* Prodrugs of a 1'-CN-4-aza-7,9-dideazaadenosine C-nucleoside leading to the discovery of Remdesivir (GS-5734) as a potent inhibitor of respiratory syncytial virus with efficacy in the African green monkey model of RSV. *J. Med. Chem.* **2021**, *64*, 5001-5017.

[11] Jun Liang; *et al.* Lead optimization of 4-aminopyridine benzamide scaffold to identify potent, selective, and orally bioavailable TYK2 inhibitors. *J. Med. Chem.* **2013**, *56*, 4521-4536.
[12] Toru Taniguchi; *et al.* Discovery of novel pyrido-pyridazinone derivatives as FER tyrosine kinase inhibitors with antitumor activity. *ACS Med. Chem. Lett.* **2019**, *10*, 737-742.
[13] Ted W. Johnson; *et al.* Discovery of (10R)-7-Amino-12-fluoro-2,10,16-trimethyl-15-oxo-10,15,16,17-tetrahydro-2H-8,4-(metheno)pyrazolo[4,3-h][2,5,11]-benzoxadiazacyclotetradecine-3-carbonitrile (PF-06463922), a macrocyclic inhibitor of anaplastic lymphoma kinase (ALK) and c-ros oncogene 1 (ROS1) with preclinical brain exposure and broad-spectrum potency against ALK-resistant mutations. *J. Med. Chem.* **2014**, *57*, 4720-4744.
[14] Joachim Broker; *et al.* Fragment optimization of reversible binding to the switch II pocket on KRAS leads to a potent, in vivo active KRAS G12C inhibitor. *J. Med. Chem.* **2022**, *65*, 14614-14629.

Sulfone in Medicinal Chemistry

The sulfone moiety has been frequently used in medicinal chemistry to optimize potency and physicochemical properties. There are several examples of approved drugs and clinical candidates containing sulfone moiety (**Figure 152**). The sulfone moiety has been found to function as important pharmacophore responsible for a range of biological activities in many therapeutic areas. Its ability to confer conformational constraint, serve as hydrogen bond acceptor, and influence proximal functionality by virtue of its electron-withdrawing property has been exploited to maximize interactions with proteins in order to optimize affinity or potency. Besides, sulfone moiety can be used as one of ketone isosteres that offers increased polarity while avoiding the potential for ketone reduction, and as one of carboxylic acid isosteres that is devoid of the burden of the charge of the carboxylate. In addition, sulfone moiety is very polar that can lower the overall lipophilicity and improve aqueous solubility and metabolic stability of a molecule, which can lead to an overall improvement of ADMET. [1]

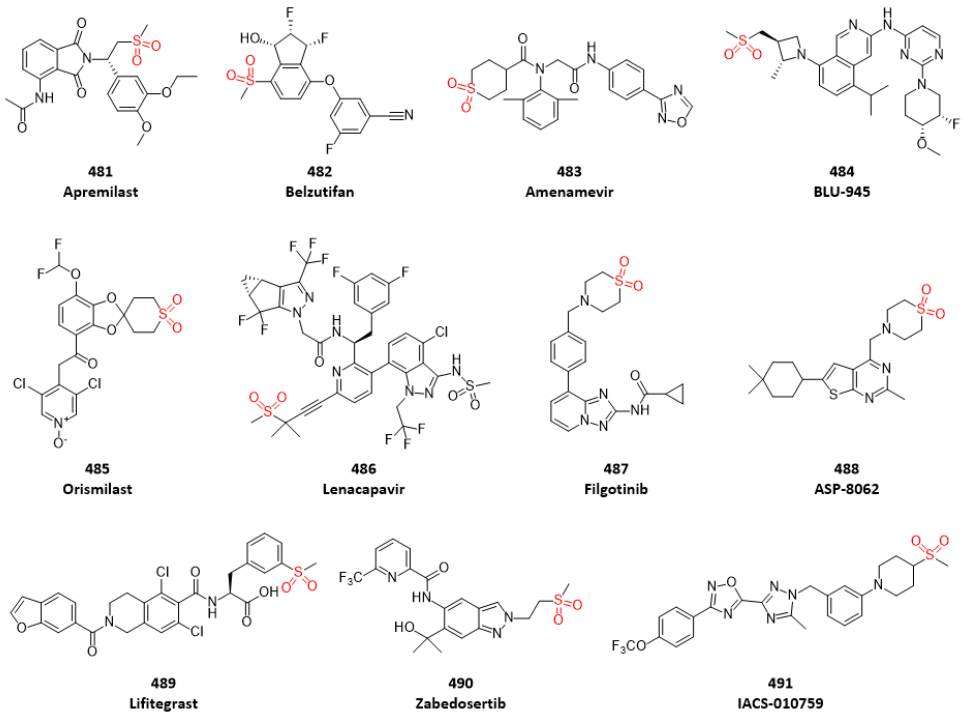

Figure 152. Approved drug and clinical candidate molecules containing sulfone

In the course of discovery of **BLU-945** (compound **484**), a reversible, potent, and wild-type sparing next generation EGFR mutant inhibitor for the treatment-resistant non-small cell lung cancer, compound **492** was identified as a potent and selective lead compound. However, compound **492** suffered a low metabolic stability in human microsome. To address this problem, it was identified that 3-position of the azetidine ring was a vector to explore the addition of polar substituents to tune properties. Among of substituents explored by the team, sulfone-containing compound **493** was distinctly superior, with excellent stability in human microsome and increased potency compared to compound **492**. In order to explain observed potency increasing, X-ray crystal structure of compound **493** bound to EGFR LR/TM revealed that this improvement could be attributed to two hydrogen bonds between sulfone moiety and two Lys716 and Lys728 in the front pocket of protein (**Figure 153**). [2] Further optimization based on compound 493 led to discovery of **BLU-945** (compound **484**).

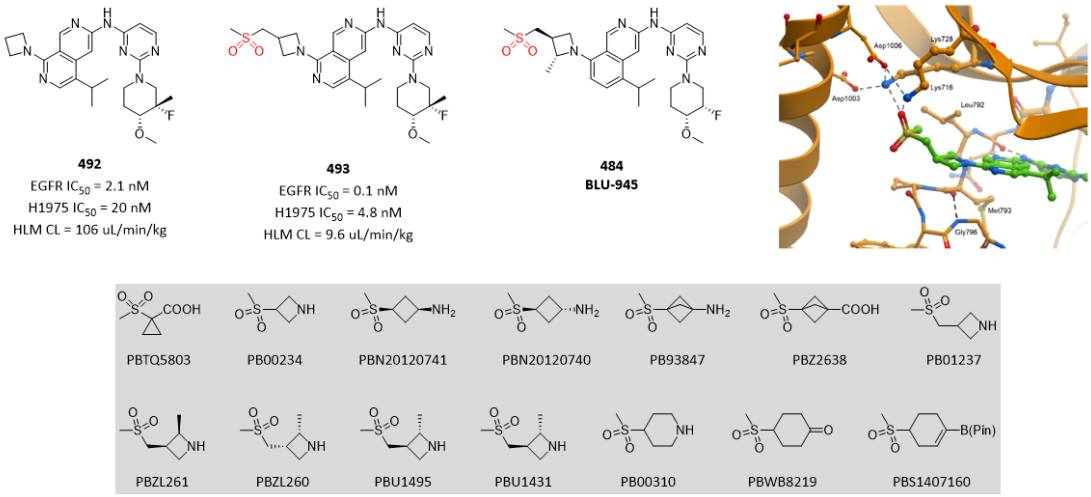

Figure 153. Sulfone moiety increased both metabolic stability and potency. (PDB code: 8D76)

In order to increase ATAD2 potency and selectivity against BRD4 of hit compound **494**, several analogues with increased polarity were synthesized and evaluated. The most promising compound **496** containing sulfone moiety achieved this goal. To better understand the interactions made by the cyclic sulfone, X-ray crystal structure of compound **496** bound to ATAD2 was obtained. There are two polar interactions made by the two sulfone oxygen atoms, each of which accepts hydrogen bonds from the guanidinium group of Arg1077 (**Figure 154**). [3]

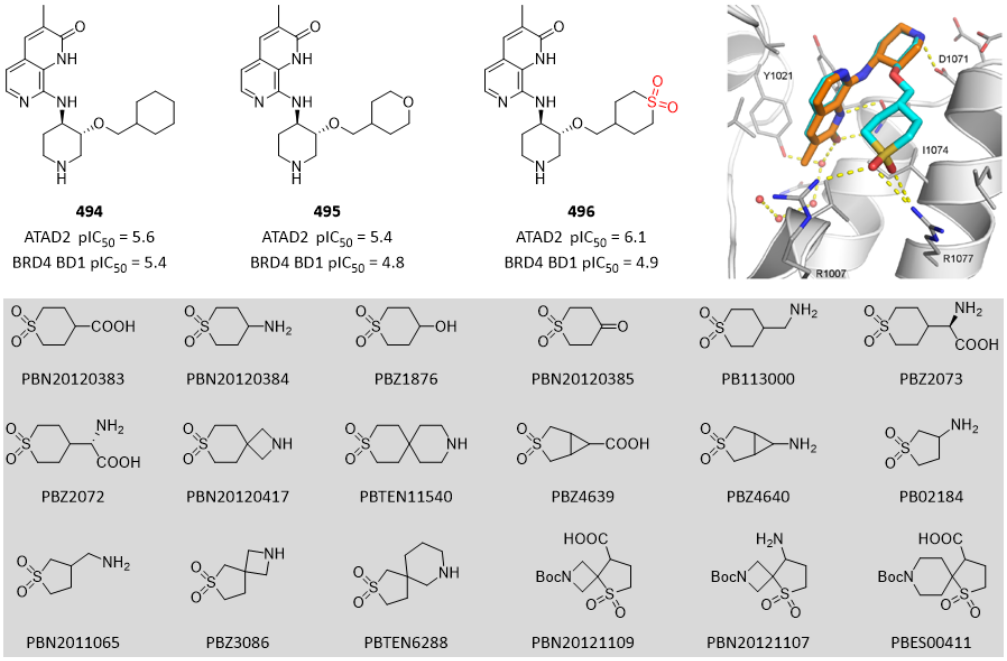

Figure 154. Sulfone moiety increased both potency and selectivity. (PDB code: 5A82)

The enhanced selectivity over BRD4 of compound **496** relative to compound **494** is due to both increased ATAD2 potency and decreased BRD4 activity. The ATAD2 potency gain arises from the new direct hydrogen bonds to the arginines and the displacement of the weakly bound water molecules. The reduction of BRD4 activity presumably results from placing polar sulfone oxygen atoms in an unfavorable lipophilic location. The tetrahydropyran compound **495** is intermediate in polarity between the compound **494** and compound **496**, and shows intermediate selectivity.

Compound **497** was identified as a novel, potent V1b antagonist. However, this compound suffered a high *in vivo* clearance. To address this critical issue, several polar moieties were introduced into

molecules, as exemplified by compound **498** and compound **499** (**Figure 155**). The in vivo clearance was well consistent with polarity of oxygen atom and sulfone moiety. [4]

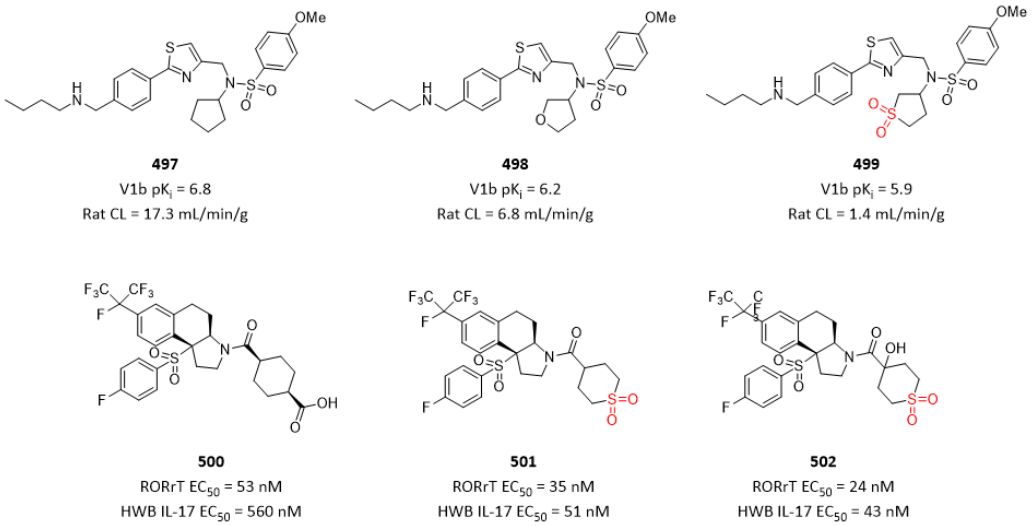

Figure 155. Sulfone moiety improved physicochemical properties of molecules due its high polarity.

Comparing compound **500** and compound **501**, as RORgammaT antagonists, sulfone moiety increased human whole blood potency by at least 10-fold, although both compounds have similar enzymatic RORrT potency. This is probably due to poor permeability of carboxylic acid in compound **500**. Therefore, cyclic six-membered sulfone can be used as one excellent surrogate for carboxylic acid (**Figure 155**). [5]

Piperidine ring often causes hERG inhibition due to basicity of nitrogen. To address this problem, electron-withdrawing atom(s) are introduced, as exemplified by difluoropiperidine, morpholine, etc. Due to the most electron-withdrawing property of sulfone, thiomorpholine dioxide is less basic than morpholine and difluoropiperidine. Therefore, thiomorpholine dioxide is often used when reduction of basicity is desired and specially when avoiding hERG inhibition liability (**Figure 156**).

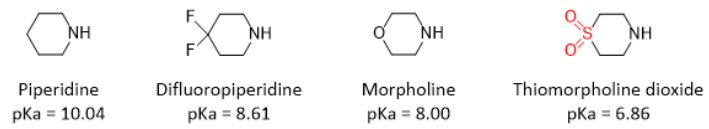

Figure 156. Comparison of pKa values (calculated by ChemDraw software)

Compound **503** was a potent, selective CB2 receptor agonist. However, this compound inhibits hERG with 88% inhibition at 100 uM. As described above, hERG ion channel is well known for its preference of ligands with a basic amine group. To address this issue, general strategies were employed to reduce basicity of nitrogen of piperidine by introducing a fluorine atom in compound **504**, introducing two fluorine atoms in compound **505**, replacing piperidine with morpholine in compound **506** and replacing piperidine with thiomorpholine dioxide in compound **507**. The extent of decreasing hERG inhibition is consistent with the ability of reducing basicity of nitrogen atom (**Figure 157**). [6]

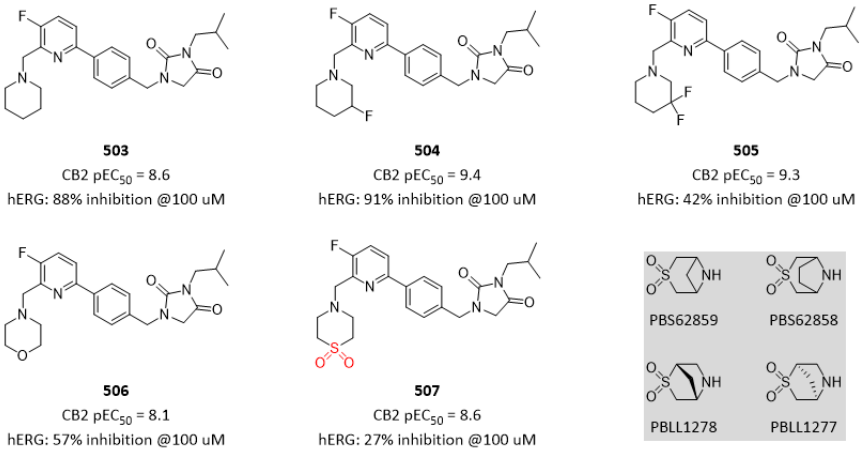

Figure 157. Sulfone moiety in thiomorpholine dioxide decreased hERG inhibition.

In the course of discovery of **Filgotinib** (compound **487**) as a JAK1 selective inhibitor, it was found that replacing morpholine in compound **508** with N-methyl piperazine in compound **509** lost potency completely, while sulfone moiety in **Filgotinib** (compound **487**) increased both potency and metabolic stability in rat liver microsome. X-ray crystal structure of **Filgotinib** (compound **487**) bound to JAK2 revealed that the terminal thiomorpholine dioxide group packs against the glycine rich loop, forming polar interactions with main chain atoms of this flexible loop (Gly861, Ser862), the side chain of Val863, and the catalytic Lys882 and Asp994 of the DFG segment (**Figure 158**). [7]

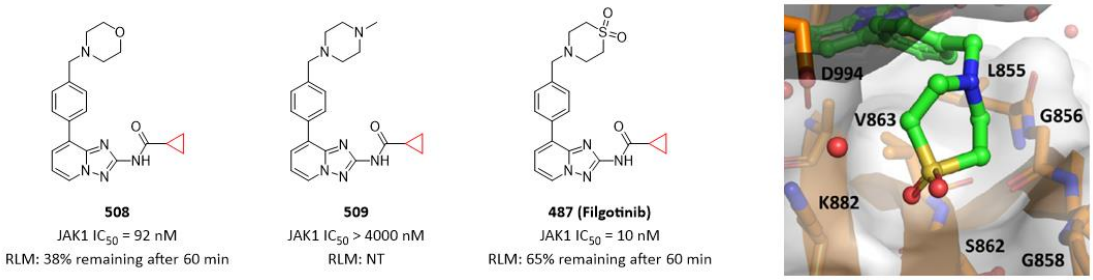

Figure 158. Sulfone moiety increased both potency and metabolic stability. (PDB code: 4P7E)

References

[1] Alicia Regueiro-Ren. Cyclic sulfoxides and sulfones in drug design. *Advances in Heterocyclic Chemistry* **2021**, *134*, 1-30.
[2] Meredith S. Eno; *et al.* Discovery of BLU-945, a reversible, potent, and wild-type-sparing next-generation EGFR mutant inhibitor for treatment-resistant non-small-cell lung cancer. *J. Med. Chem.* **2022**, *65*, 9662-9677.
[3] Paul Bamborough; *et al.* Structure-based optimization of naphthyridones into potent ATAD2 bromodomain inhibitors. *J. Med. Chem.* **2015**, *58*, 6151-6178.
[4] Chris A. Smethurst; *et al.* The characterization of a novel V1b antagonist lead series. *Bioorg. Med. Chem. Lett.* **2011**, *21*, 92-96.
[5] David Marcoux; *et al.* Rationally designed, conformationally constrained inverse agonists of RORrT-identification of a potent, selective series with biologic-like in vivo efficacy. *J. Med. Chem.* **2019**, *62*, 9931-9946.
[6] Mario van der Stelt; *et al.* Discovery and optimization of 1-(4-(pyridine-2-yl)benzyl)-imidazolidine-2,4-dione derivatives as a novel class of selective cannabinoid CB2 receptor agonists. *J. Med. Chem.* **2011**, *54*, 7350-7362.

[7] Christel J. Menet; *et al*. Triazolopyridines as selective JAK1 inhibitors: from hit identification to GLP0634. *J. Med. Chem.* **2014**, *57*, 9323-9342.

About Author

Jin Li

Senior Director

10+ years' experience in organic chemistry
3+ years' experience in medicinal chemistry
10+ patents and papers published
Inventor of 2 clinical candidates
Email: li_jin@pharmablock.com

Contact Us

PharmaBlock Sciences (Nanjing), Inc.
Tel: +86-400 025 5188
Email: sales@pharmablock.com

PharmaBlock (USA), Inc.
Tel(PA): +1(877)878-5226 Tel(CA): +1(267) 649-7271
Email: salesusa@pharmablock.com

Find out more at www.pharmablock.com

Official Website Product Search Wechat LinkedIn